Landmarks in Earth Reinforcement, - Ochiai et al (eds),
© 2003 Swets & Zeitlinger, Lisse, ISBN 90 265 1863 3

Long-term performance and seismic stability of reinforced soil structures reported in Japan

O. Murata
Railway Technical Research Institute

T. Uchimura
University of Tokyo

K. Ogata & S. Tayama
Japan Highway Public Corporation

E. Ogisako
Shimuzu Corporation

K. Kojima
Railway Technical Research Institute

J. Nishimura
Mitsui Chemical Industria, Ltd.l

M. Hirata
Toyo Construction Co., Ltd

H. Miyatake
Public Work Research Institute

ABSTRACT: Several reports on researches and observations on long-term performance and seismic stabilities of reinforced soil embankments and reinforced slopes are introduced. Based on authors' survey on more than 200 reports mainly published in Japan, some trends of the present knowledge and techniques on these topics are pointed out.

1 INTRODUCTION

The first modern method of soil reinforcement, the Terre Armée, has been used and developed for more than 30 years, while soil reinforcement methods by using geosynthetics have been used for almost 20 years. Meanwhile, many research projects on soil reinforcement, including static, cyclic and seismic loading tests on small scale and full scale models, have been performed. Loading tests and long term observations also have been performed on real construction projects of reinforced soil structures. Based on the results from these researches and experiences, several practical design and construction methods have been developed. In addition, the observation results on reinforced soil structures in the severely damaged sites of the Hyogoken-Nambu Earthquake in 1995, Japan, have shown their very high seismic stability.

In this paper, researches and observations on long-term performance and seismic stabilities of reinforced soil embankments and reinforced slopes, mainly reported in Japan, are introduced. The authors hope that these reports will be useful for engineers and researchers who are executing new researches and observations, and developing new design and construction methods on reinforced soil structures in the next generation.

2 LONG-TERM PERFORMANCE AND SEISMIC STABILITY OF REINFORCED SOIL EMBANKMENTS

2.1 *Outline of reinforced soil embankments*

Reinforced soil embankments are designed and constructed to have improved quality in strength, stiffness and/or drainage properties by laying metal or synthetic reinforcement in a shape of bar, sheet or grid on each compacting layers in construction. Figure 2.1.1 shows typical structures of reinforced soil embankments. Some of them are called reinforced soil walls if they have steep (or perpendicular) slopes. Surface of some slopes are wrapped-around by the reinforcement as shown in Figure 2.1.1 (b), and some walls have more rigid slope structure such as concrete panels or full-height reinforced concrete facings as shown in Figure 2.1.1 (c).

Bearing capacity and long-term consolidation property of the foundation grounds, the backfill compaction quality control, and the backfill deformation problems are necessary to be considered in design and construction. The deformation and failure potential near the slope or the wall surface also should be checked, especially under strong seismic conditions. From the viewpoint of long-term performance, chemical and mechanical stability and de-

terioration properties of the reinforcement materials are important, although the history of soil reinforcement technique is not long enough to verify these problems. Because the behaviours of the backfill, the reinforcements and the facings are very complicated and interacting with each other, the mechanism of the structure behaviours are not understood completely yet, and researches are still going on. Several very simplified design methods are used in practical works at present.

2.2 *Long-term performance*

2.2.1 *Summary*

In the practical design works at present, the potential failure of the structures caused by the self-weight and assumed external forces is mainly verified. However, stability and deformation potential during the long service period are not verified quantitatively, and reasonable and effective methods for such verification are not yet established.

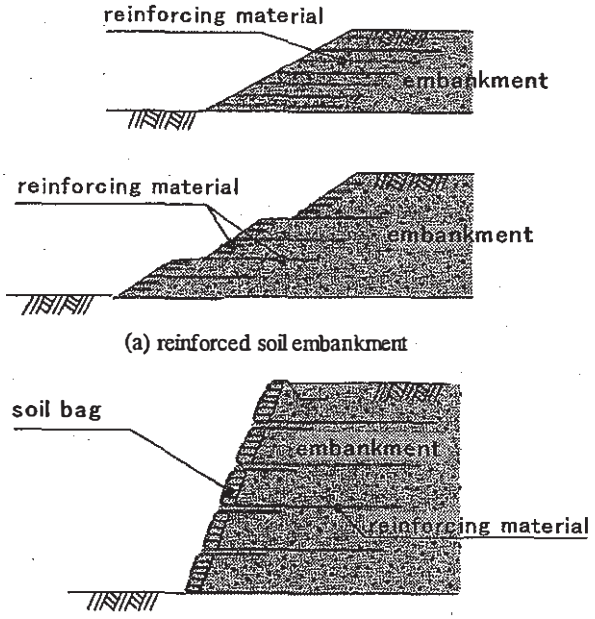

(a) reinforced soil embankment

(b) reinforced soil wall (without concrete wall)

(c) reinforced soil wall (with concrete wall)

Figure2.1.1 Types of reinforced soil embankment

Important factors which affects the long-term performance of reinforced soil structures are the creep deformation of the backfill and reinforcement materials, their residual deformation caused by long-term and/or cyclic loading in service, deformation of the foundation ground caused by consolidation and creep, deterioration of the materials, very severe rainfalls and seismic forces which are possible during the service periods, and etc.

Accumulation of data from careful long-term observations of reinforcement soil structures are essential for developing methods to consider such factors in design. The measurement items in usual observation are vertical displacements of top, intermediate layers and the foundation ground, lateral displacements of wall and slope surface, developing strains in the reinforcement, earth pressures at the back face of the facings, pore water pressures in the backfill, and etc. In most of long-term observations reported to the public, their measurement periods are several weeks to several months limited within the construction periods, and the behaviours after construction and during service were observed in only few cases.

2.2.2 *Case studies*

An observation of a reinforced soil structure under long-term cyclic traffic load is presented. Such long-term observation of effects of traffic load in service is very few among more than 200 report which TC9 has searched from existing publications in Japan. An investigation on corrosion problem in metal reinforcements after more than 25 years of service is also presented.

(1) *Residual compression of PLPS grid-reinforced soil pier caused by traffic load*

Preloaded and prestressed (PLPS) reinforced soil method aims at making a reinforced backfill very stiff against vertical load by vertical preloading and prestressing. The first prototype PLPS geogrid-reinforced soil bridge pier was constructed to support a pair of temporary railway girders, each 16.5 m in length, in the summer of 1996 in Fukuoka City, Japan (P1 in Figure 2.2.1) (Uchimura et. al. 1998). This pier was opened to service since from 1997 to 2001.

Before constructing the pier, a subsoil layer of an about 9 m-thick very soft clay was improved by cement-mixing method. The lower ends of four steel tie rods were anchored into the cement-mixed soil columns for a length of 4 m. Then the backfill was constructed with a help of gravel-filled bags stacked along the periphery of each gravel layer, while the bags were wrapped around with the reinforcement. A well graded gravel of crushed sandstone was used for the backfill. A geogrid reinforcement of polyvi-

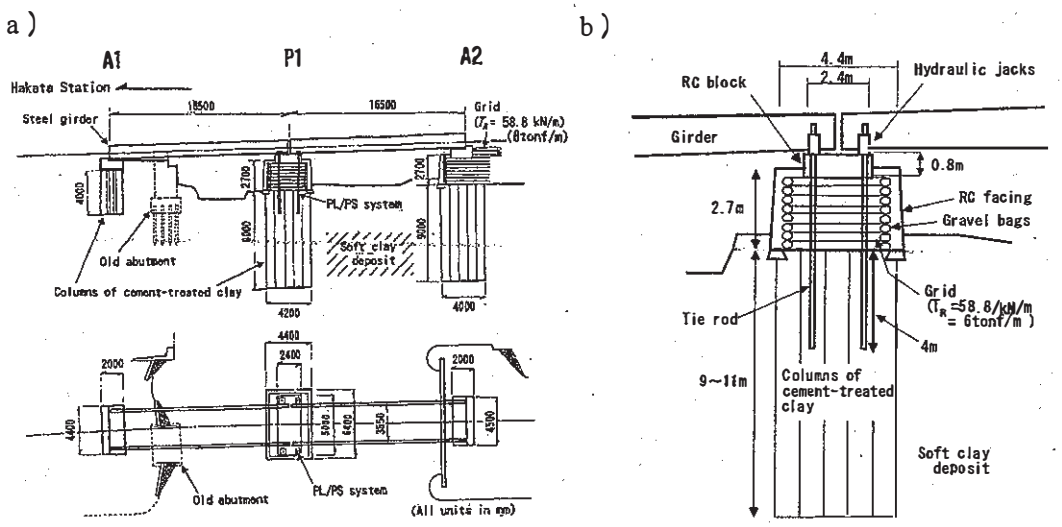

Figure 2.2.1 a) Maidashi bridge with PLPS reinforced soil pier at the center; and b) details of the pier

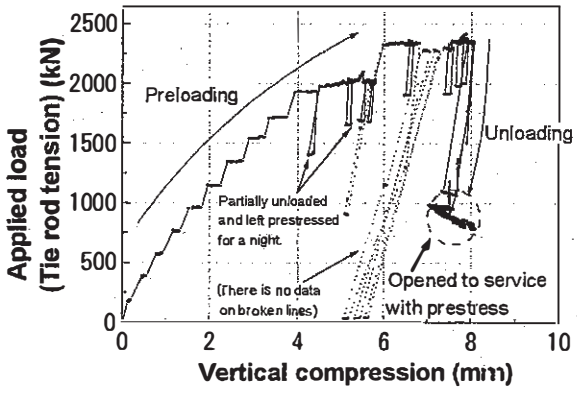

Figure 2.2.2 Compression of the pier by preloading

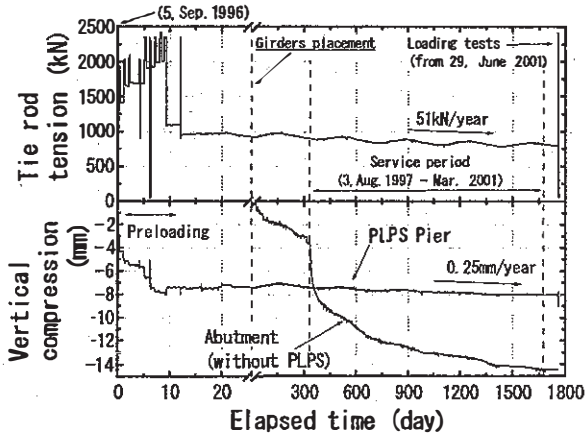

Figure 2.2.3 Long-term time histories of tie rod tension and vertical compression of the pier and abutment

nyl alcohol coated with polyvinyl chloride (PVC) was used with an average vertical spacing of 15 cm.

Preloading started ten days after casting the top reaction RC block with maximum preload of 2400 kN (an average vertical pressure of 200 kPa) to the

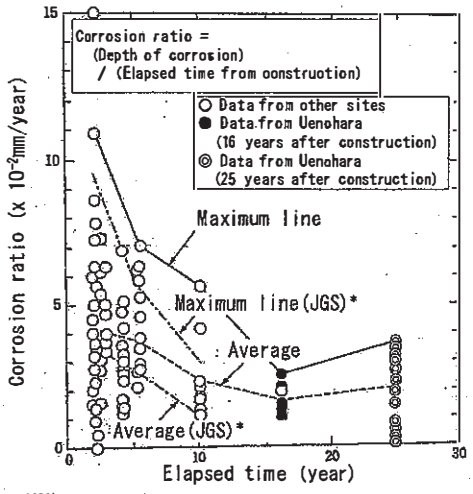

(JGS)* :
After investigations by Japanese Geotechnical Society.
Corrosion ratio were measured for 126 Samples of L-shaped steel bars embedded at 10 sites in Japan.

Figure 2.2.4 Corrosion ratios of metal strips.

backfill of the pier through the top reaction block by using four hydraulic jacks installed at the top of the tie rods (Figure 2.2.2). The backfill was compressed by 8 mm during preloading. Then the load was reduced to 970 kN, and the top ends of the tie rods were fixed to the top RC block to maintain the compressive stress (i.e. prestress) in the backfill. Finally, full-height rigid facings were cast-in-place around the backfill.

On the other hand, the abutment A2 (Figure 2.2.1) has been constructed as an ordinary-type geogrid-reinforced soil abutment, which was neither preloaded nor prestressed. Its design and material were the same as the PLPS pier, except that it has only one GRS retaining wall having reinforcement with a vertical spacing of 30 cm, without PL and PS, and the both sides are exposed slopes (1.5:1.0 in H:V) without facings.

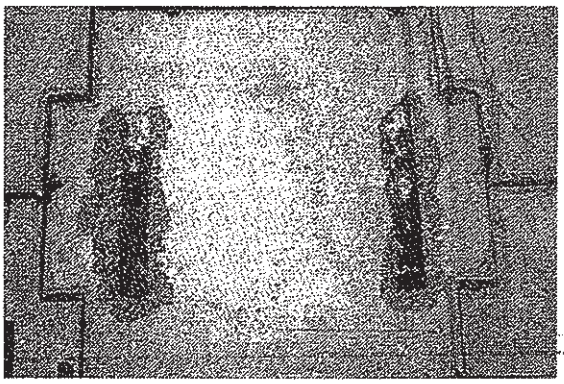

Figure 2.2.5 Skin before remedy work

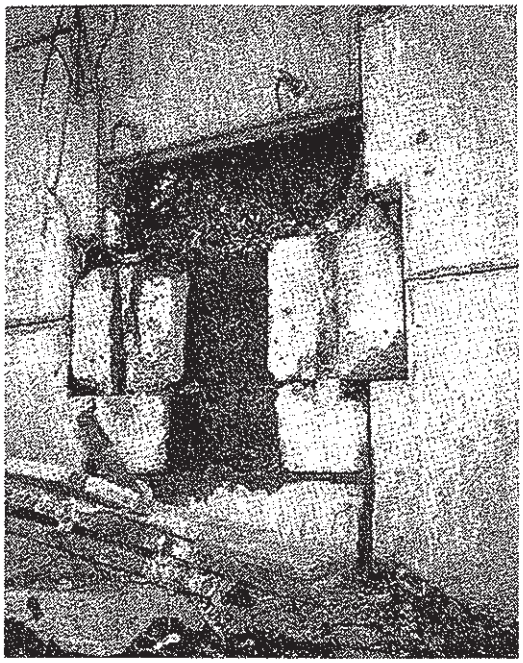

Figure 2.2.6 Cut and removed skin.

The vertical compression and the tie rod tension of the pier P1 and the abutment A2 have been observed for more than 4 years after construction (Figure 2.2.3). After being compressed by about 8 mm for the first 10 days of preloading period, the PLPS pier was compressed very slowly under the prestressed condition. Even after being opened to service, the compression rate of the pier kept to a very small value, and the tie rod tension decreased only very gradually. These rates of change are small enough for a temporary use for about 5 years. On the other hand, the abutment, without PL and PS, was compressed very quickly after opening to service. The compression is still continuing after more than 4 years. These comparisons show that the preloading and prestressing procedure is very effective to reduce vertical compression of the reinforced backfill.

(2) *Corrosion of metal reinforcements for walls*

Corrosion process of reinforcing bar (metal-strip reinforcements) for the reinforced soil wall, which was constructed for a highway embankment in Uenohara region in 1972 has been observed for more than 25 years. The wall is the first reinforced soil wall in Japan. In 1988, an observation was performed for those bars, and some of the skins were found to be partially detached, while some of the connective strips were exposed and corroded.

In 1997, about 25 years after the construction, the following investigations were performed (Tonogaito et. al. 1998):

i) Several skins were removed and the corrosion conditions of the metal bars and the concrete were observed. The detachment of the concrete on the skin was found where the thickness of the concrete on the connective strip is less than 1.5 cm. This detachment can be consider to be due to too small concrete thickness. The minimum thickness is defined in the design code at the present. As for the skins without detachment, the concrete was proved to be in a good condition, and the reinforcements of the skin concrete were not corroded.

ii) Several metal bars were sampled by using boring machine. The upper surfaces of the bars were corroded for a length of 50 cm from the skin, and the rusty materials were found in the backfill soil above the bars. On the other hand, the lower surfaces of the bars were not corroded. Figure 2.2.4 shows the corrosion ratios versus the elapsed time after construction (Wakatsuki et. al. 1989). The corrosion ratio is defined as the depth of corrosion (total of the both sides) per the elapsed time after laying the bars. Herein, the data from the investigation mentioned above is also plotted.

iii) Several skins were removed, and the alignments of the metal bars were observed. The bars were tilting by about 5 degrees so that the farther ends from the skin were lower than the initial places. Near the skins, there were spaces between the lower surface of the bars and the backfill soil. These displacements are possibly due to the settlement of the backfill, and the backfill can be considered to have settled more than the skins.

After those investigation mentioned above, the following trial remedy process were performed (Kawai et. al. 1998):

i) A skin whose concrete surface had been detached and the connective strips were exposed, was chosen for the trial remedy work (Figure2.2.5).

ii) Four holes with diameter of 60 mm were made through the skin, and chemical stabilization materials were injected between the skin and the backfill in order to prevent failure of the backfill. Two more holes were made through the skin in order to

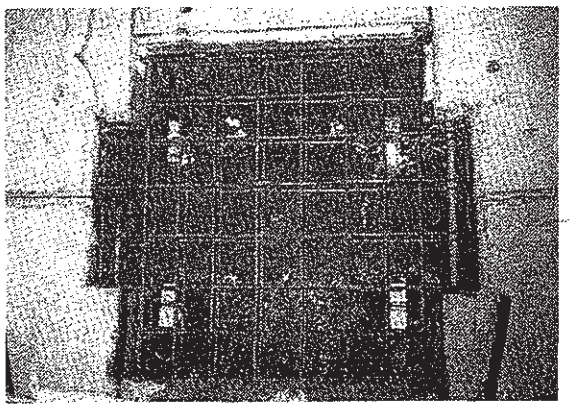

Figure 2.2.7 Assembled connective strips

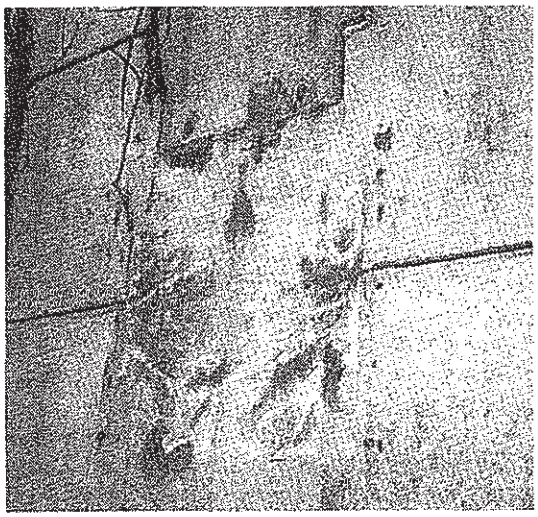

Figure 2.2.8 Skin after remedy work and reinforcement for skin concrete.

check the grouting conditions.

iii) The skin was cut into 9 parts by using a concrete cutter, and removed by hammers (Figure 2.2.6).

iv) Existing connective strips, the bolts and the nuts were removed, and new T-shaped connecting strips were connected to the metal bars. The reinforcements were assembled for the new skin. Soft materials were put along the joints to adjacent skins to avoid the effects of volume changes of the fresh concrete (Figure 2.2.7).

v) A mold for the new skin was assembled, which was supported by anchors drove into the adjacent skins, and concrete was cast in place (Figure 2.2.8).

2.2.3 Numerical analysis

Most of numerical analysis of the field constructions are two-dimensional (plane strain) analysis by finite element method. There are many types of reinforced soil embankment with geosynthetics, reinforcing bars, or steel meshes. In many cases the reinforcements are modeled as truss elements and joint elements are set between the soil and the reinforcements. The various constitutive laws, such as elastic, elasto-plastic, etc., are used for the soils. Most analysis simulates the behaviors during the construction period only, and in very few cases a consolidation or a creep phenomena is considered.

Two examples of analysis results for reinforced soil embankments are introduced below.

(1) *Reinforced soil wall with clay foundation*

A clayey soil embankment, approximately 100m wide, 1800m long, and 2m high, was constructed for a train yard for Hokuriku Bullet Train in Nagano. Its west side slope was built as geosynthetic-reinforced soil walls with rigid facing as shown in Figure 2.2.9 (Kojima et al. 1996).

The foundation ground of this site is very soft clay layer, over 30m deep, in Quartenary Alluvium deposit. It was expected that a large deformation will occur in the clay and peat layers with N-value of nearly equal zero. The ground water level is very high (G.L.-45cm) and the wet density of soil is 1.2g/cm^3 with a porosity ratio of 5. A preloading procedure was taken by constructing an embankment 2.5m-high with slopes of 1:1.5.

A clayey material was used for the backfill. Therefore an increase of a pore water pressure in construction is expected. As the countermeasure, a composite material of a non-woven geosynthetics with a drainage effect and a woven geosynthetics with a reinforcing effect was used. Figure 2.2.10 shows the structure of the material.

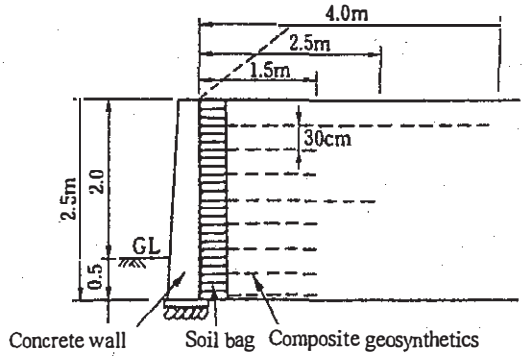

Figure 2.2.9 Cross-section of embankment

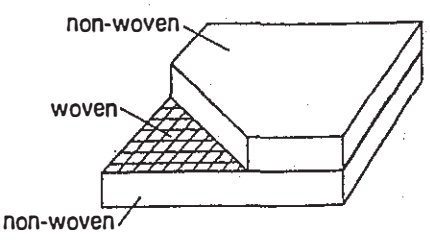

Figure 2.2.10 Composite geosynthetics

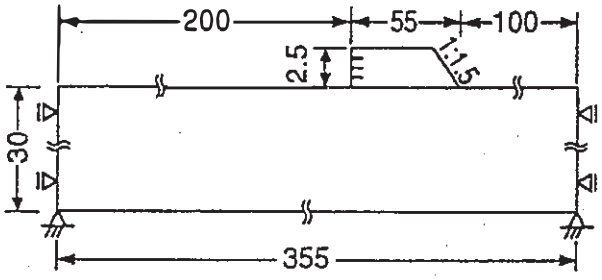

Figure2.2.11 Analytical model

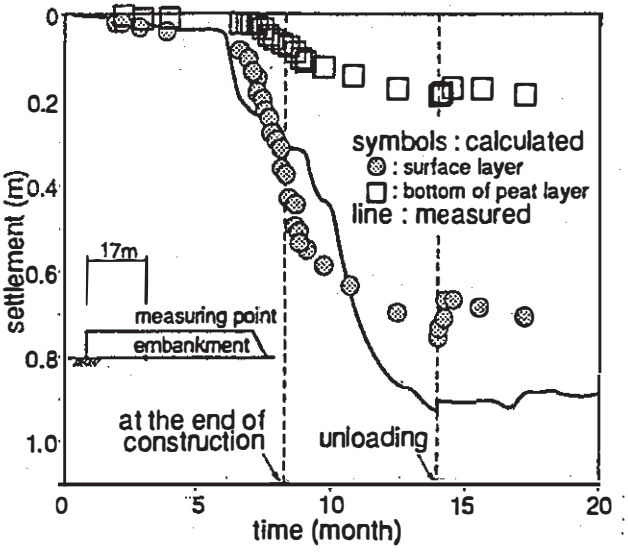

Figure2.2.12 Settlement of ground

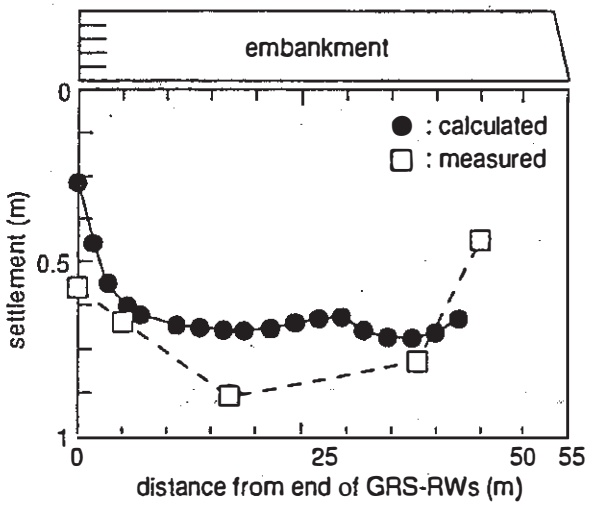

Figure2.2.13 Distribution of settlement of ground surface

Based on the results of the analysis and the measurement for the preloading process, the deformation of the ground during the embankment construction was analyzed by finite element method (Kojima et al. 1996). The soil/water coupling elasto-viscoplastic analysis with a constitutive equation of Sekiguchi-Ohta model was used because the materials for both of the ground and the embankment were cohesive soils. The soil parameters used in analysis were mainly determined from the uni-axial compression tests. Figure 2.2.11 shows the model of the analyzed structure. The reinforcement is modeled as a truss element and the hydraulic boundary condition was set along the reinforcement. The analysis results of settlement-time curves are shown in Figure 2.2.12. Figure 2.2.13 shows the analyzed settlement of ground surface as viewed in cross-section. The analyzed values of the settlement are a little smaller than the measured value. However the tendency of settlement can be reasonably estimated by the analysis. The reason of the small difference may be that the characteristics of a surface layer could not be properly estimated.

(2) *Reinforced soil embankment using box-type wall*

Behaviors of a geogrid reinforced soil wall using box-type wall for a highway embankment was measured during its construction from June 24th to the end of December in 1997. The measured items are the earth pressure, the deformation of the ground, the strain in the geogrids, the pore water pressure and the displacement of the wall. Their behaviors were analyzed by elasto-plastic finite element method (Shinowki et al. 1998).

The foundation soil was lava bed of the central crater of Mt. Aso and most of the ground are the deposits of volcanic ash. A box-type walls made by concrete block, whose size are 1m high and 2m wide with its weight of 12.7kN in each, were used for the wall structure. The mountain muck was used for the backfill, while the single-grained macadam was used behind the wall blocks. Geogrid was used in order to reduce the earth pressure acting on the wall as shown Figure 2.2.14.

An elasto-plastic finite element method was used for the analysis. The Drucker-Prager model was used as the constitutive law of soil, and the reinforcements were modeled as truss elements with joint elements introducing the frictional property into its shear stiffness between the soil and the reinforcement. The ground was modeled as three layers, that is, volcanic ash silt, silt with gravel, and cohesive soil with gravel. The joint elements are set between earth and mountain muck, and between mountain muck and macadam. The self-weights of the embankment layers were applied step by step.

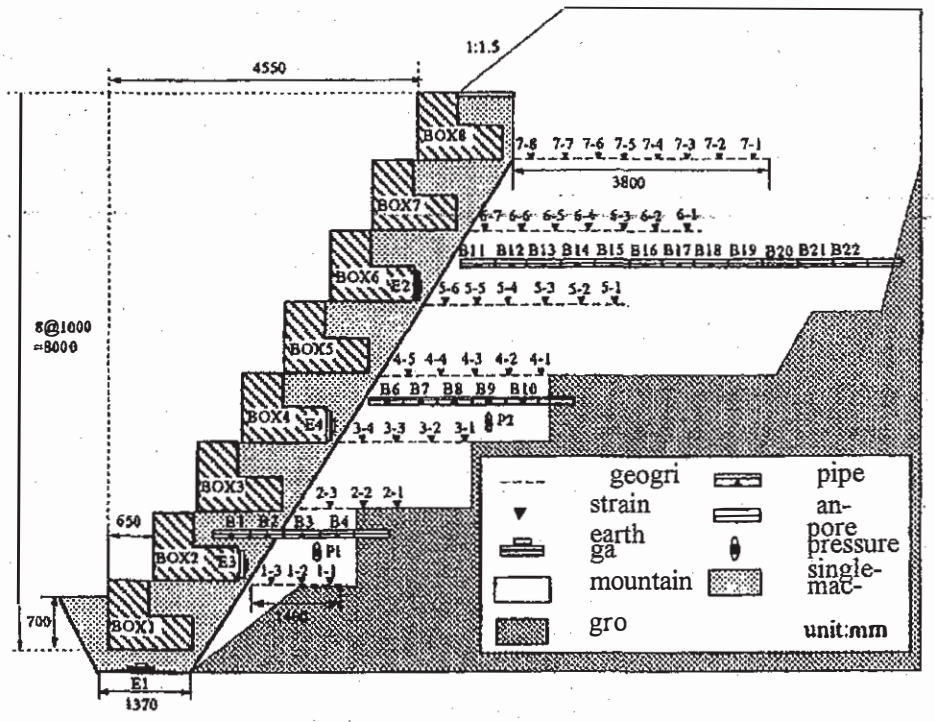

Figure2.2.14 Cross-section of embankment

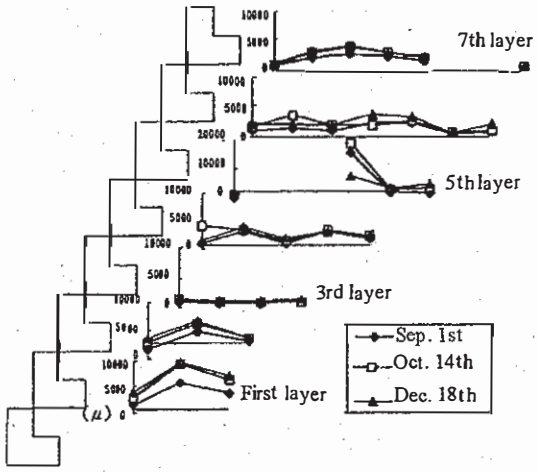

Figure2.2.15 Distribution of strain in geogrid (measurement)

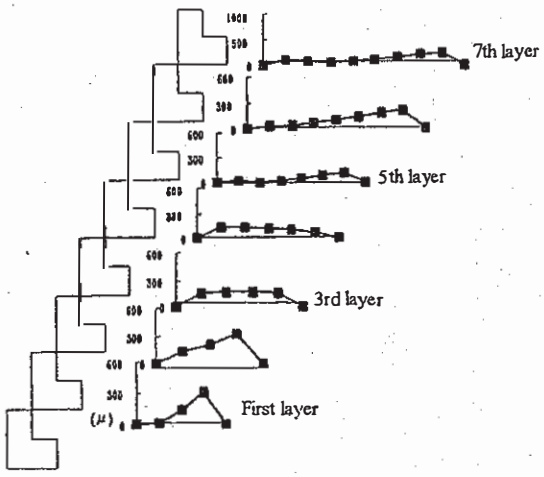

Figure2.2.16 Distribution of strain in geogrid (analysis)

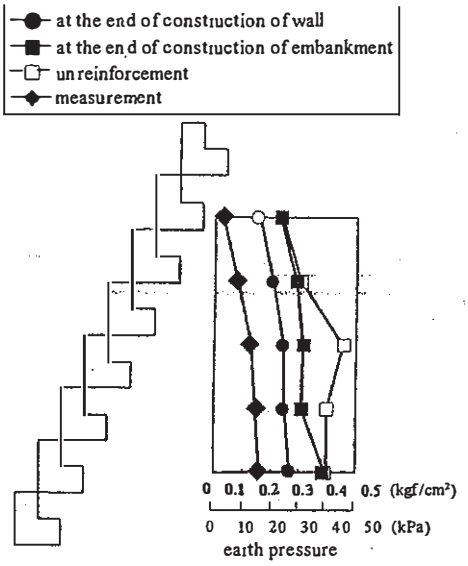

Figure2.2.17 earth pressure in horizontal direction

Figure 2.2.15 shows the distribution of the measured strain in each geogrid. The strain increases as the construction proceeds, and it becomes consistent after the completion of the total height of embankment. The strains at No.1 and No.2 layers are relatively larger than those of other layers and the peak values clearly appear for those two layers. On the other hand, the strains at from No.3 to No.7 layers except of No.5 layer are almost uniform. It can be considered that the reinforcing material at the lower part of embankment is effective to reduce the earth pressure. Figure 2.2.16 shows the distribution of the strain in each geogrid by analysis. Almost the same tendency as the measurement is observed, except that the magnitude of analytical values are relatively smaller than those of measured values. Figure 2.2.17 shows the distribution of the earth pressure in horizontal direction by analysis. The transition of the earth pressure as the proceeding of the construction is expressed well and its shape of distribution is almost the same as the measurement although its magnitude is different. In the same figure, the analysis result of an unreinforced case is shown. The effects of the reduction of earth pressure by reinforcing material appear clearly and the effectiveness of this method is proved.

REFERENCES

Uchimura,T., Tatsuoka,F., Tateyama,M., Koga,T.: Preloaded-Prestressed Geogrid-reinforced Soil Bridge Pier, *Proc. the 6th Int. Conf. on Geosynthetics*, Atlanta, Vol.2, pp.565-572, 1998.

Tonogaito, M., Kawai, Y., Nishi, T. and Oohiro, Y. : Site investigation for durability of the Terre Armée method, *Proc. of the 33id Japan National Conference of Geotechnical Engineering*, Vol. 2, pp. 2423-2424, 1998. (in Japanese)

Kawai, Y., Matsuzawa, K., Kobayashi, K. and Nishi, T. : Replacement of Damaged Concrete Facing Panels on a Reinforced Earth Structure, *Proc. of the 33id Japan National Conference of Geotechnical Engineering*, Vol. 2, pp. 2425-2426, 1998. (in Japanese)

Wakatsuki, Kawaragawa, Okuda : Pull-out Test In-situ in Reinforced Earth Walls, Research Institute Report, *Nihon Doro Kodan (Japan Highway Public Corporation)*, Vol. 26, 1989. (in Japanese)

Kojima, K., O. Murata, O. Maruyama & T. Yonezawa : Geosynthetic-reinforced soil retaining wall using cohesive soil, The Foundation Engineering & Equipment, Vol.24, No.12, pp.64-67, 1996.12

Kojima, K., N. Sakamoto, M. Tateyama & O. Maruyama : Geosynthetic-reinforced soil retaining wall using clay on a very soft ground for Hokuriku bullet train yard in Nagano, *Proc. of Int. Symposium on Earth Reinforcement*, 1996.11

Shinowaki, S., J. Otani, and T. Hirai : Field measurements and numerical analysis of box-type retaining wall reinforced by geosynthetics, *Proc. of the 33rd Japan National Conference of Geotechnical Engineering*, Vol. 2, pp.2413-2414, 1998.7 (in Japanese)

2.3 *Seismic stability of reinforced soil embankments*

2.3.1 *Summary*

Extensive researches on seismic stability of earth structures have been conducted in Japan, because Japan has frequent earthquakes. In the 1995 Hyogoken-Nambe Earthquake, it had been confirmed that reinforced-soil structures could withstand against seismic force. The present seismic design methods are based on medium-scale earthquake motion (L1 earthquake motion) and limit equilibrium design are being adopted in accordance with the seismic intensity regulation.

Limit equilibrium design is possible to determine the stability of structures against destruction, but unable to say anything on structural deformations (facing, crest, etc.) which are attributable to other causes than destruction. Therefore, it is desirable to adopt rational designs which may allow certain deformations in large-scale earthquakes (L1 earthquake motion). Under such circumstances, it will be necessary to consolidate all related past experiments and researches to promote further studies, with due consideration to performance assessment design and critical state design method.

The authors have surveyed more than 100 reports related to seismic study on reinforced soil structures published in Japan. As a result, the followings can be summarized on the experimental methods conducted at the present:

1) Most of the experiments are conducted by limited researchers or institutes using the same experimental equipment systematically;

2) Most of the experimental methods use shaking tables (including centrifugal gravity) with small-scale models;
3) The experiments essentially aim at understanding destruction/deformation modes, and the evaluations of their results are based on relative comparison.

Because variety of the target of the researches on this topic is limited, it may be rather easy to construct fundamental concepts in order to proceed with related researches. It seems possible to set up 'Universal Platform' defining terms, measuring items, modes of phenomena, fundamental ideas, etc., as a standard of experimental research methods.

In the following section, several reports on reinforced soil embankments and retaining structures damaged by the 1995 Hogoken-Nambu Earthquake and the 1999 Chi-Chi earthquake in Taiwan, as well as an investigation of a geotextile-reinforced embankment during the Tottori earthquake are introduced.

2.3.2 *Case studies of Recent Earthquakes*

1) *The 1995 Hyogoken-Nambu Earthquake*

i) *Reinforced-soil retaining wall for railway (Tatsuoka et. al. 1997)*

A geogrid-reinforced soil retaining wall, with a maximum height of 6.2m, had been constructed using RRR (Reinforced Railroad/Road with Rigid facing) method in a severely damaged site of the 1995 Hyogoken-Nambu Earthquake (Figures 2.3.1). Although the maximum ground acceleration at the site is estimated to have been so high as 0.7g, and the length of the installed geogrid was rather short, no major damage was recognized except a slight inclination of the retaining wall.

Six concrete-retaining walls in the same region were surveyed, and back-analyses were conducted based on detailed soil quality investigations. The results showed that back-calculated seismic intensity values at both the reinforced-soil retaining walls and concrete-retaining walls were lower than the actually measured values of the ground surface. Therefore, it was pointed out that the current seismic intensity value (kh=0.15) must be raised when earthquakes as strong as 1995 Hyogoken-Nambu Earthquake are taken into account from the standpoint of design. Also, the following factors are conceivable for inconformity between seismic intensity and accelerated speed on the surface ground:

- Soil quality constant used by stable calculation method and design;
- Consideration of effects by wall facing;
- Kinetic effects;
- Allowable safety factor; etc.

a)

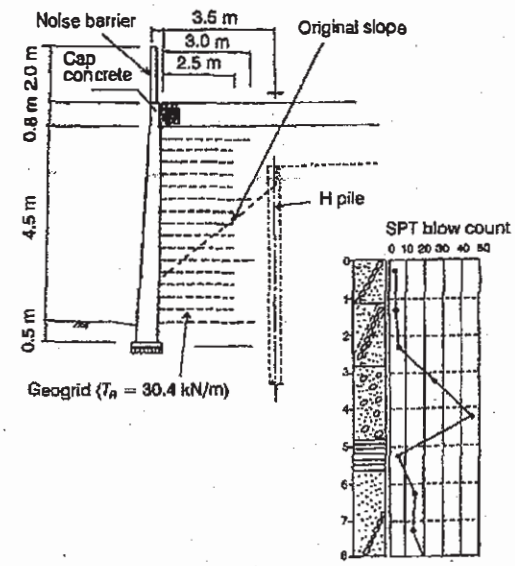

b)

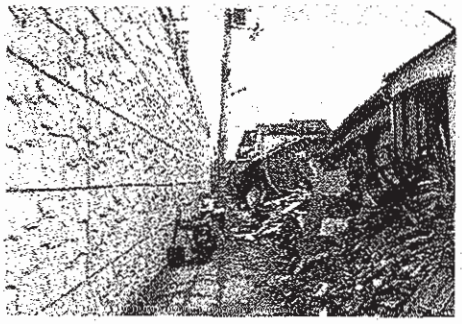

Figure 2.3.1 a) Typical cross section of a GRS-RW, and b) Side view showing collapsed wooden houses

Among the kinetic effects, it seems that inconsistency of seismic tremor and frequency characteristics are important factors.

ii) *Walls for highway embankments*

Ten geosynthetic-reinforced soil retaining walls constructed at sites whose estimated maximum ground acceleration are 0.3g to 0.7g had been surveyed (Figures 2.3.2. and Table 2.3.1.) (Nishimura et. al. 1996). No damage, including minor deformation, was recognized in most of the walls. However, liquefaction of the base ground and corresponding slight deformation of conventional concrete block retaining walls were noticed in two of the surveyed walls. Compared to the serious damages of other retaining structures at adjacent areas, geosynthetic-reinforced soil walls have suffered only minor damages without losing their functions.

Back analyzed seismic intensity based on the present design method was 0.1～0.4. As a result, it is evaluated that the subject reinforced soil walls could withstand against seismic loads having maximum acceleration speeds exceeding those of designed seismic intensity plus gravity.

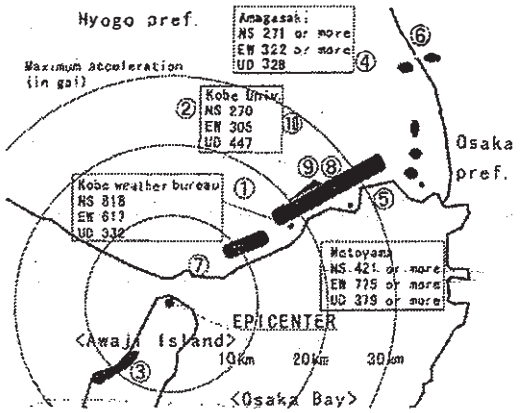

Figure 2.3.2 Location of the Geogrid-reinforced soil walls

2) *The Chi-Chi earthquake of September 21,1999 (Koseki et. al. 2000)*

Because the epicenter of the Chi-Chi earthquake, 1999, was in the mountain area, a number of concrete-retaining walls constructed on mountainous roads was severely damaged. The importance of the foundations for retaining walls, especially on the steep slopes, was pointed out.

It was also recognized that several geogrid- reinforced soil retaining walls constructed with small non-reinforced concrete blocks (20cm high/per blocks) piled up for the facings, with a height of 2.8 ~3.5m, were damaged (Figure 2.3.3 and 2.3.4). It was found that the intensity of the damage was related to the installation of the geogrid as follows:

i) Where the geogrid were installed at intervals of 60cm : No damages;
ii) Where the geogrid were installed at an interval of 80cm : Partially collapsed;
iii) Where the geogrid were installed at an interval of 120cm : Swelling at the lower part (It was likely that the damaged degree differed depending upon the existence of the facing)
iv) Where the backfill was not reinforced (only H-shaped steel bars were installed behind the facing) : Collapsed

A four-stage reinforced-embankments constructed on a excavated slope, about 40m-high in total, was collapsed (Figure 2.3.5). The facing of the each stage was constructed by piling up about 10 sandbags, which were wrapped up with the geogrids. The reinforcements were placed with intervals of 80 to 100cm (Figure 2.3.6). The essential reasons for this large-scale collapse were considered as follows:

i) The installation intervals of the reinforcement were too large, causing a great earth pressure on the lower sandbags, which resulted in partial destruction. Due to the same reason, the restraining effect of the reinforcement for horizontal tensile strain of the embankment was reduced, resulting in insufficient compaction at the installation time conceivable.
ii) Where the wrapping up length of the reinforcing materials was not sufficient, the reinforcing materials were slipped out of the embankment even with slight deformation, which resulted in losing the reinforcement's restricting effect of deformation of the sand bags. The resulting partial collapse triggered off total destruction of the embankment.

Table 2.3.1 Structure of the investigated geogrid-reinforced soil walls

No.	Completion of Construction	Facing	Geogrid	Reinforcement length (m)	Height of Wall (m)	Inclination	Internal friction angle (deg)	Observation
1	Jun. 1990	Steel frame	SR55	4.8	6.5	1:0.1	30	No damage
2	Feb. 1991	Concrete block	SR55	3.0	4.0	1:0.3	30	No damage
3	Aug. 1991	Sandbag	SR55	5.5	6.2	1:0.5	30	No damage
4	Feb. 1992	Sandbag	SR55	5.0	6.6	1:0.3	30	No damage
5	Mar. 1993	Concrete block	SR55	4.5	5.25	1:0.5	30	Small gaps between concrete blocks and a few centimeters settlement
6	Dec. 1993	Sandbag	SR80	7.5	11.0	1:0.3	30	No damage
7	Jul. 1994	Steel frame	SR55	2.0	5.0	1:0.5	35	No damage
8	Aug. 1994	Sandbag	SR35	4.0	5.5	1:0.2	30	A crack ran parallel to wall face on the crest because of unstable foundation
9	Sep. 1994	Sandbag	SR35	3.5	5.0	1:0.0	30	No damage
10	Dec. 1994	Sandbag	SR80	5.5	5.0	1:0.3	30	No damage

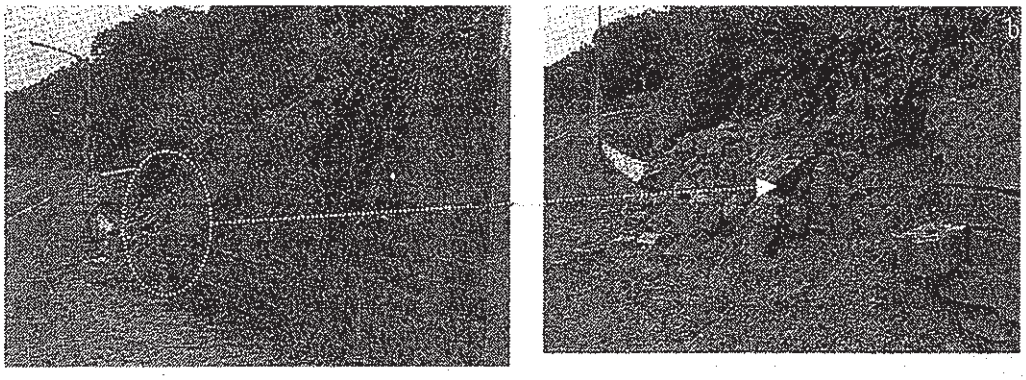

Figure 2.3.3 Damage to a reinforced-soil retaining wall using block-type facing

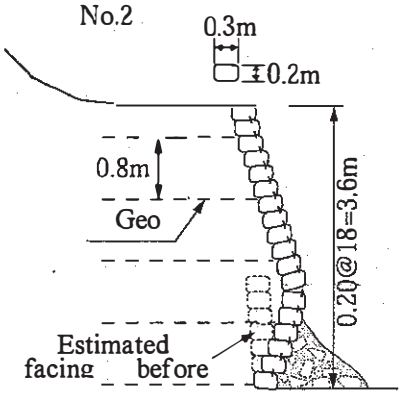

Figure 2.3.4 Cross-section of the damaged reinforced-soil retaining wall using block-type facing

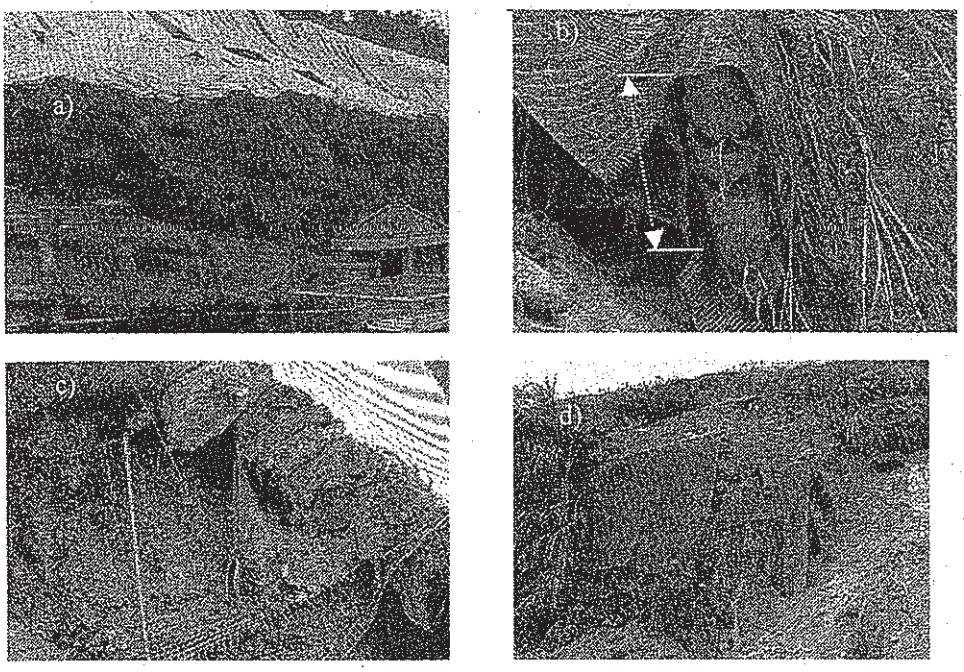

Figure 2.3.5 Damage to wrapped-around type reinforced-soil embankment

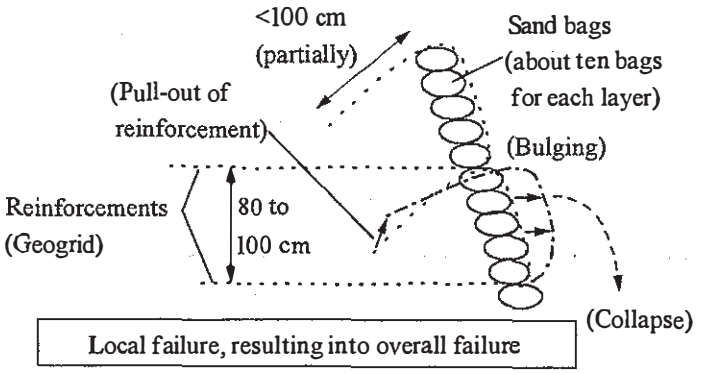

Figure 2.3.6 Schematic figure on damage to wrapped-around type reinforced soil embankment.

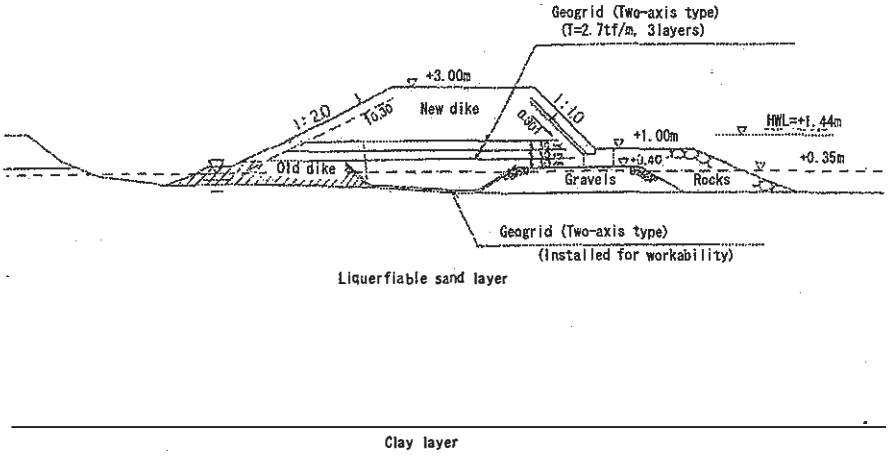

Figure 2.3.7 A typical cross-section of dike with reinforced foundation

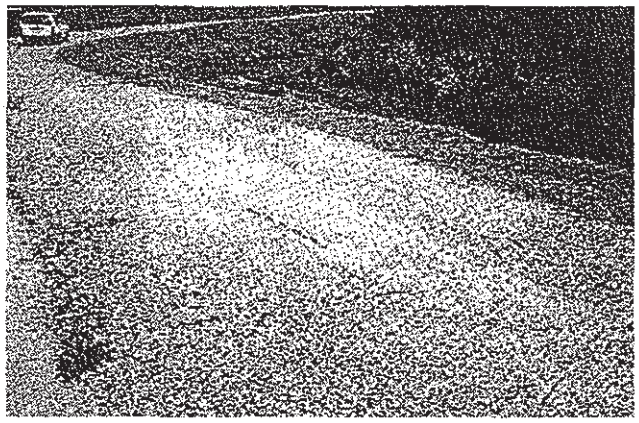

Figure 2.3.8 A transversal crack observed on top of the dike.

(3) *Tottori Seibu Earthquake*

In line with a repairing project of the 'NAKAUMI-SHORE' in ~~TOTTORI / SHIMANE~~ prefectures, an investigation of the ground had been conducted for the purpose of constructing a new embankment with a height of about 3m (Sasaki and Funato, 2001). As a result, it was found that there was an accumulated soft sand layer with a depth of 7 to 8 m on the shallow ground above the base ground on which the embankment was surrounded by farm lands and the geogrid-reinforcement method was ~~embankment in case of an earthquake refer to Fig~~ure2.3.7. In October 2000, after about 4 years from the completion of the embankment, the Tottori Seibu earthquake of M7.3 occurred and a maximum accelerated speed of 200 gal hit the region. However, almost all the embankment was in good condition although some minor damage was noticed in Figures2.3.8.

2.3.3 *Model tests on seismic stability*

1) *Shaking table tests for Segment-Method Reinforcing-Soil Wall*

In this chapter, a series of model shaking table tests conducted by Mr. Matsuo, et al at the Civil Engineering Research Center of The Land & Infrastructure Ministry are reported (Saitoh et. al. 1997, Tsutsumi et. al. 1997, Saitoh et. al. 1998). Figure 2.3.9 shows cross sections of the model tests.

A model of reinforcing-soil retaining wall was made using wooden partition panels as a facing with a height of 0.2m and width of 4.0mm. Reinforcing

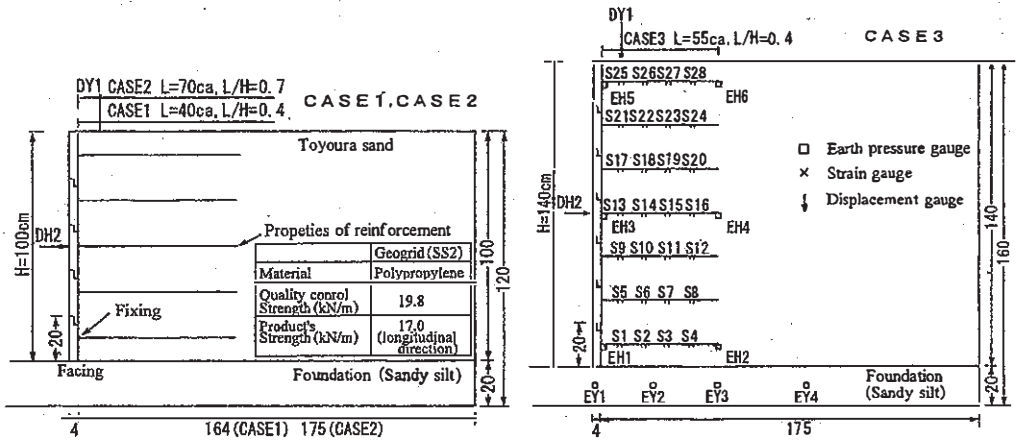

Figure 2.3.9 Cross section of the model

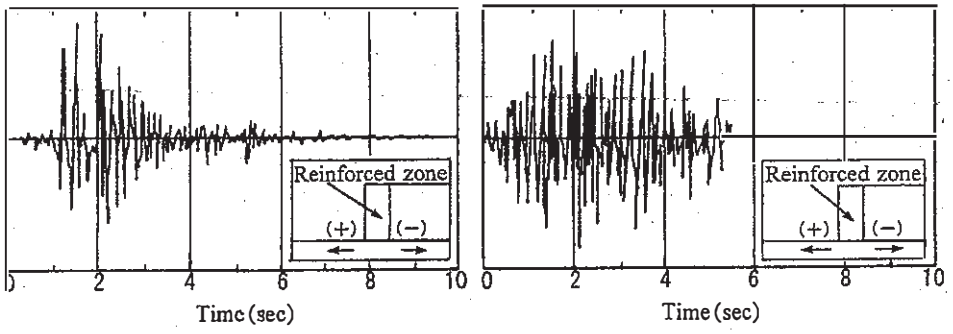

(a) Kobe wave (case7) (b) Aomori wave (case9)

Figure 2.3.10 Adopted acceleration

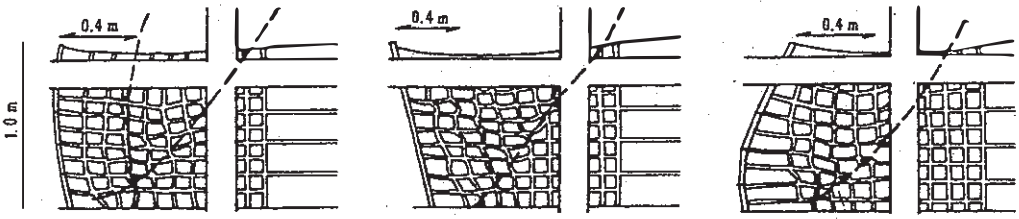

Figure 2.3.11 Deformed model reinforced soil wall

Table2.3.2. Shaking conditions

CASE	Input wave	Wall height (m)	Wall type	Grid length / wall height	Slope inclination
1	Sine wave	1.0	Separated panels	L/H=0.4	Perpendicular
2	Sine wave	1.0	Separated panels	L/H=0.7	Perpendicular
3	Sine wave	1.4	Separated panels	L/H=0.4	Perpendicular
4	Kobe wave	1.0	Separated panels	L/H=0.4	Perpendicular
5	Sine wave	1.0	Full height rigid	L/H=0.4	Perpendicular
6	Sine wave	1.0	Separated panels	L/H=0.4	1:0.2
7	Aomori wave (5Hz)	1.0	Separated panels	L/H=0.4	Perpendicular
8	Sine wave	1.0	Full height rigid	L/H=0.7	Perpendicular
9	Kobe wave (5Hz)	1.0	Separated panels	L/H=0.4	Perpendicular

materials (tensile strength 1.5tf/m) were installed at intervals of 0.2m. An embankment was compacted by a 0.1 m / layer so that Toyoura sand at an air-dried state would become dry density of ρ_d=1.50g/cm^2(Dr≒60%)

In the subject experiments, the followings were changed (Table 2.3.2) :

- Installation length of the reinforcing material;
- Embankment height;
- Facing rigidity;
- Embankment Shape; and
- Seismic motion type.

In Case 5 and Case 8, partition panels on the facing were fixed using a rigid reinforcing-board. Input waves were:

- Case4 : N-S were (Kobe wave) measured at the Hyogoken-Nambu Earthquake;
- Case7 : Kobe wave; and
- Case9: N-S wave (Aomori wave) measured at TOKACHI-OKI Earthquake was adjusted so that excellence-frequency would become 5Hz.

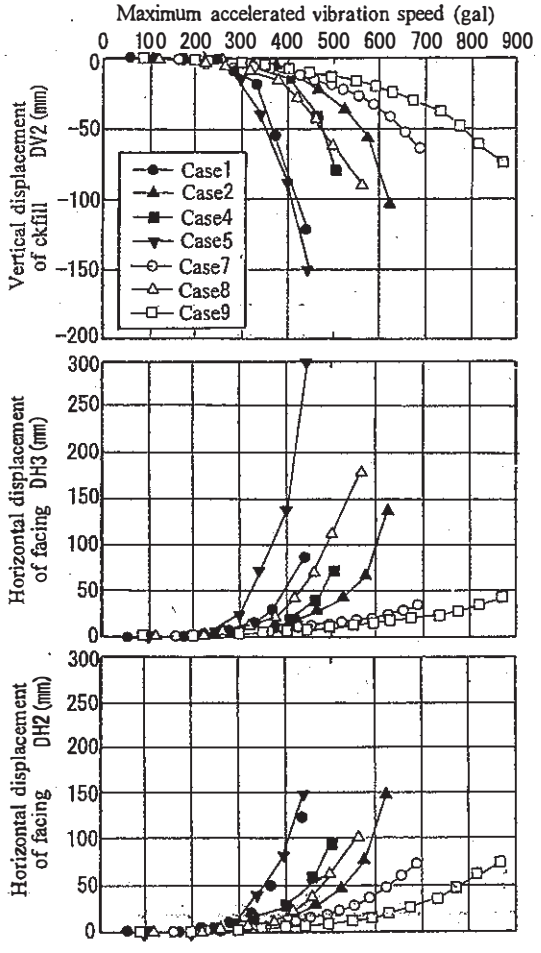

Figure 2.3.12 Relationships between maximum accelerated vibration speeds, settlements and horizontal deformation of facing

Refer to Figures 2.3.10. The acceleration speeds were increased by stages. Deformed model embankments are shown in Figures 2.3.11. Sliding took place from the outside of reinforced area toward the lower part of reinforced area along with the reinforcing material. While start of sliding occurred at 350 gal in Case 1, which was at 550 gal in Case 2 where the distance of reinforcing material installation was long. Deformed models of each Case were compared:

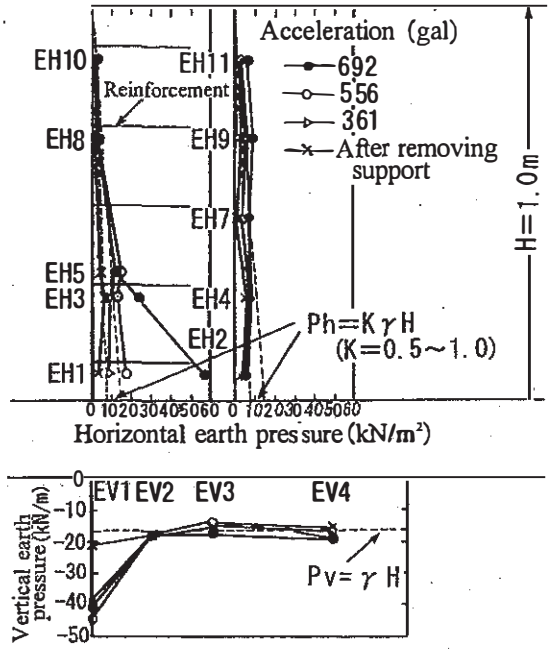

Figure 2.3.13 Maximum earth pressure distribution during vibration (Case 7)

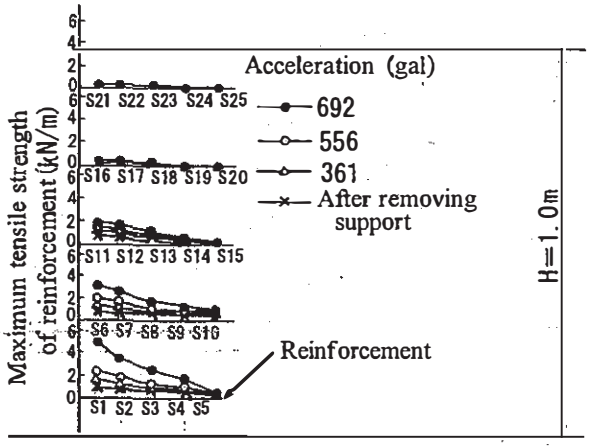

Figure 2.3.14 maximum tensile distributions during vibration (Case7)

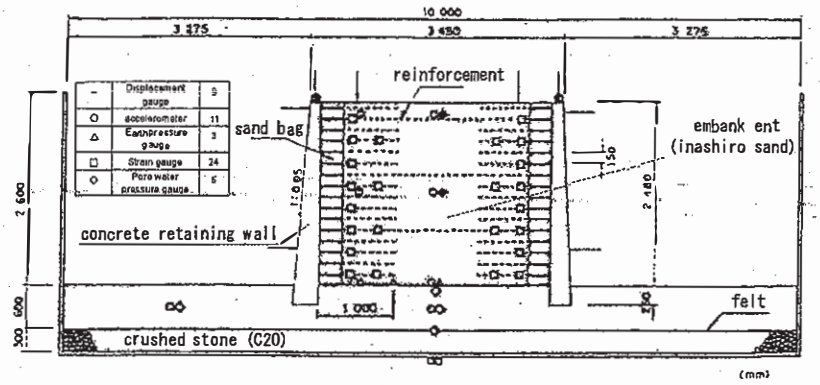

Figure.2.3.15 Cross-section of GRS-RW model and location of gauge installed

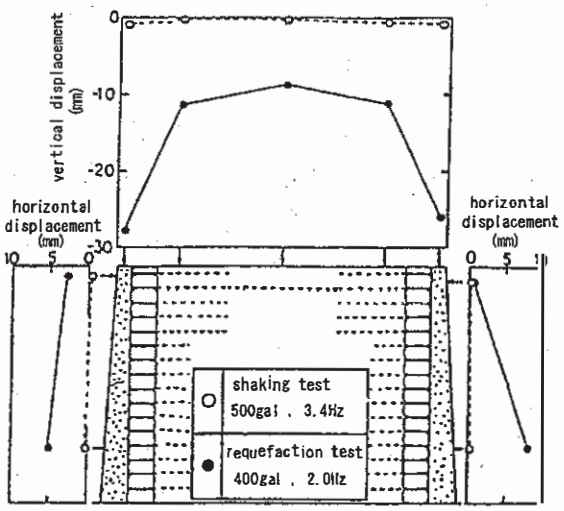

Figure.2.3.16 Horizontal and vertical deformation of retaining wall

- In the partitioning wall, the reinforced area was bulged in the forward direction and dropped in wedge-shape in the backward direction;
- In the one-piece wall, the upper top of embankment was inclined in the forward direction;
- In Case 6 where its facing had inclination deformed in a circle shape centering the upper top of facing.

Figure 2.3.12 shows relationship between maximum accelerated vibration speeds and embankment settled volumes / horizontal deformation of facing.

Deformation of one-piece walls was bigger than that of partitioning walls, which meant the stability of partitioning walls was high. When vibration was increased using seismic wave, its deformed volume was smaller than that of sinusoidal wave.

Figures 2.3.13 show maximum pressure distributions during vibration increases. In all cases, the horizontal earth pressures in the ground increased as its depth deepened. In the same depth, the earth pressure of facing was greater than that of the back side of reinforced area.

Figure 2.3.14 shows maximum tensile distributions affecting reinforcing materials during vibration increases. In all cases, the tensile strength of reinforcing materials was taking place corresponding to horizontal earth pressures effecting facing.

2) *Shaking table tests of the RRR method*

Tateyama,et.al. (1990) performed shaking table tests on the RRR method with using a large shaking table. The geosynthetic-reinforced soil retaining wall (GRS-RW) model, 2.48m-high, 3.45m-wide, with scaling of 1/2 of full-scale embankment was constructed. The fiber net (maximum extension strength 10kN/m) was used for the reinforcement material, which placed at intervals of 0.15m of the backfill. Figure 2.3.15 shows the outline of GRS-RW model. Shaking conditions in the experiment are listed in Table 2.3.3.

Figure 2.3.16 shows the experiment result of horizontal and vertical deformation of retaining wall (RW). In the shaking table tests, maximum displacement was about 1mm; there was practically no deformation. This result shows that this type of rein

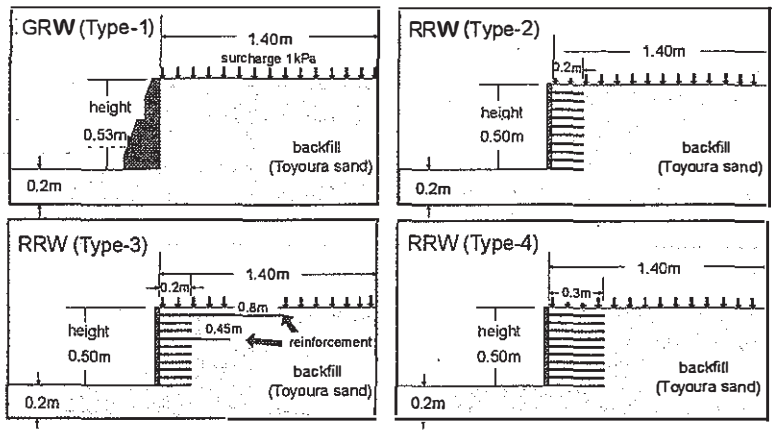

Figure.2.3.17 Cross-sections of RW models

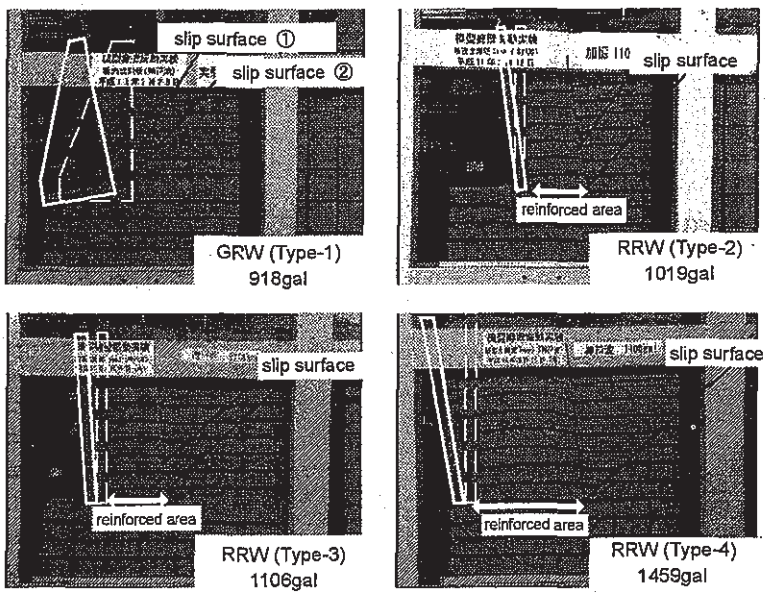

Figure.2.3.18 Deformation of the retaining wall models observed after in the shaking table tests

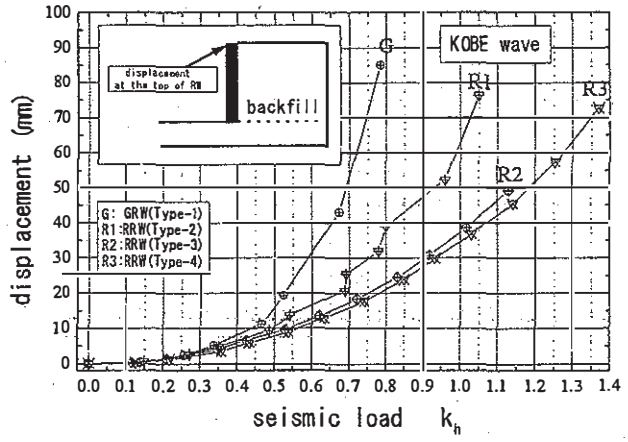

Figure.2.3.19 Relationship between the displacement at the top of RW and the seismic load "k_h"

forced soil structure has a very high resistance to earthquake. In the liquefaction tests, the vertical displacement of 8mm and the horizontal deformation of 28mm were observed at the top of RW. However, the backfill settlement was almost uniform (about 1 1mm), which suggests that the whole of the backfill behaved as a rigid body.

Watanabe,et.al .(1999) performed tilting and shaking table tests to examine the seismic stability of four types of RRR structures. Type-1 was gravity RW and Type-2, 3 and 4 were reinforced RWs, as shown in Figure2.3.17. The backfill consists of dry Toyoura sand and the reinforcement used a model grid made of phosphor-bronze strips. In the shaking table test, amplitude of sinusoidal wave and irregular wave called Kobe wave that observed the 1995 Hyokoken-Nambu Earthquake were using input table acceleration.

Figure2.3.18 shows the deformation of the models observed after in the shaking table tests. See the gravity RW (Type-1) result, the slip surface occurred at the heel of retaining wall. But at the reinforced RW (type-2, 3 and 4) results, a reinforced area was unified and sheared, a slip surface occurred in the RW from that back.

Figure2.3.19 shows the relationship between the displacement at the top of RW and the seismic load "k_h". From this result, though deformation develops rapidly with the gravity RW, but the deformation doesn't develop rapidly with the reinforced RW as for the high seismic load as well, because of ductility shown in the reinforcement. This tendency agrees with the damage case by the 1995 Hyokoken-Nambu Earthquake qualitatively.

REFERENCES

Tatsuoka,F., Tateyama,M., Uchimura,T. and Koseki,J. 1997: Geosynthetic-Reinforced Soil Retaining Walls as Important Permanent Structures, *The 1996-1997 Mercer Lecture, Geosynthetics International*, Vol.4, No.2, pp.81-136.

Nishimura, J., Hirai, T., Iwasaki, K., Saitoh, Y., Morishima, M., Shintani, H., Yoshikawa, S., Yamamoto, H. : Earthquake resisitance of geogrid-reinforced soil walls based on a study conducted following the southern Hyogo earthquake *Proc. of the International Symposium on Earth Reinforcement,* pp. 439-444, 1996.

Sasaki, Y., Funato, T., : Settlements of dike reinforced by geotextiles during Tottori-seibu earthquake, *Proc. of the 16th Japanese Geosynthetics Symposium*, 2001 (in Japanese)

Koseki, J., Hayano, K., : Preliminary Report on Damage to Retaining Walls Caused by the 1999 Chi-Chi Earthquake, *Bulletin of Earth Reinforcement Structure,No.33,*.pp23-33, 2000.

Murata, O., Tateyama, M., Tatsuoka, F. : Shaking Table Tests on Embankment with Short Plane Reinforcement and Rigid Facing : *Proc. of the 25th Japan National Conference on Geotechnical Engineering,* Japanese Geotechnical Society, Vol.2, pp.2023-2026, 1990 (in Japanese)

Saitoh, Y., Matsuo, O., Tsutsuni, T. : Shaking table tests on seismic stability of reinforced soil walls -effects of wall rigidity, input acceleration waveform and wall gradient- : *Proc. of the 32nd Japan National Conference on Geotechnical Engineering,* Japanese Geotechnical Society, Vol.2, pp.2521-2522, 1997.(in Japanese)

Saitoh, Y., Matsuo, O., Tsutsuni, T. : Shaking table tests on seismic stability of reinforced soil walls –effects of input wave frequency, wall rigidity and reinforcement length, and input earthquake waveform- : *Proc. of the 33ed Japan National Conference on Geotechnical Engineering,* Japanese Geotechnical Society, Vol.2, pp.2389-2390, 1998 (in Japanese)

Tateyama, M., Murata, O. and Tatsuoka, F. : Shaking table tests on embankment with short plane reinforcement and rigid facing, *Proc. of the 25th Japan National Conference on Geotechnical Engineering,* Japanese Geotechnical Society, Vol.2, pp.2023-2024, 1990 (in Japanese)

Tsutsumi, T., Saitoh, Y., Matsuo, O. : Shaking table tests on seismic stability of reinforced soil walls –Prediction of Deformation Based on a Cumulative Damage Concept- : *Proc. of the 32nd Japan National Conference on Geotechnical Engineering,* Japanese Geotechnical Society, Vol.2, pp.2523-2524, 1997 (in Japanese)

Watanabe, K., Munaf, Y., Koseki, J., Tateyama, M. and Kojima, K. : Seismic stability of reinforced-soil retaining walls by tilting and shaking table tests, Proc. of Geosynthetics Engineering journal, Vol 14, pp.110-119, 1999 (in Japanese).

3 LONG-TERM PERFORMANCE AND SEISMIC STABILITY OF REINFORCED SLOPES

3.1 *Outline of reinforced slopes*

The purpose of the reinforced slope method is to enhance the stability of natural slopes, cut slopes and excavated slopes, and to support loads by placing many rod-shaped reinforcement members (including reinforcing bars and rockbolts) into the ground, which are comparatively short. Based on the use specific purpose, function and material of reinforcement, treatment method of slope, etc., this method is classified into three main categories, nailing, dowelling and micropiling; of them, nailing is most frequently used for the ground improvement of natural slopes and cut slopes. In Europe, nailing has been put in place since around 1970 for the ground improvement of slopes of railway tracks and roads. Nailing technique was introduced 20 years ago for the first time in Japan, and since then, has been implemented mainly for provisional works. Currently, use of nailing is spreading rapidly for diverse cases, including permanent slopes.

As shown in Figure 3.1.1, this technique consists of mainly reinforcement rods, injection material, head and slope protection, having the following features

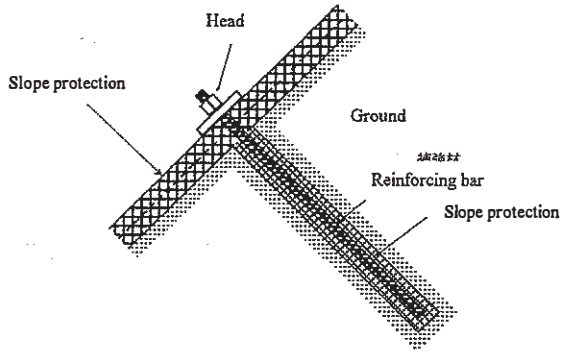

Figure 3.1.1 Basic configuration of the reinforced slope method (Japan Highway Public Corporation, 1998).

1. Possible to considerably restrain ground loosening due to excavation, by step-by-step digging and with application of reinforcement work.
2. Excellent in safety and economy, because it is possible to change the length of reinforcement rods and the distance between them by confirming the ground conditions and its alteration under excavation work.
3. Able to afford any alteration with years, by placement of additional reinforcement rods.
4. Since reinforcement rods are short and light, they can be transported even to a narrow place refusing the access of a heavy construction machine.
5. Because the technique is expected to exhibit the merits at the moment the ground starts deforming to some extent, sufficient consideration should be taken for its application when no deformation is allowed.
6. If the ground concerned is likely not to have a desired skin friction and includes a lot of places of groundwater, special attention is needed.
7. Since the main members of this method are placed underground, it is impossible to visually check the quality.

3.2 Long-term performance

3.2.1 Summary

(1) Measurement methods

The purpose of the technique is to make the ground more stable, relying on the resistance of ground reinforcement, which is designed to occur passively due to deformation of the ground. Therefore, measurement of displacement of the ground is generally conducted in order to facilitate safety management on construction work and modification of design quantity.

Measurement items for displacement may include slope top horizontal displacement, top settlement and ground displacement, with axial force of reinforcement if required. Cracks in the top and slope are checked visually.

Table 3.2.1 shows measurement items and measurement instruments for general use. The disposition of measurement instruments is shown in Figure 3.2.1 (Japan Highway Public Corporation. Oct. 1998).

Table 3.2.1 Items of displacement measurement

Measurement items	Instruments to be used
Visual checking	—
Displacement of slope top and verticality	Electro-optical distance meter, Surface extensometer
Surface displacement	Surface extensometer
Wall displacement	Electro-optical distance meter, CCD camera
Ground displacement	Borehole inclinometer
Reinforcement rod axial force	Reinforcement axial force meter, Strain gauge

*Required instruments will be added for measurement of ground water levels.

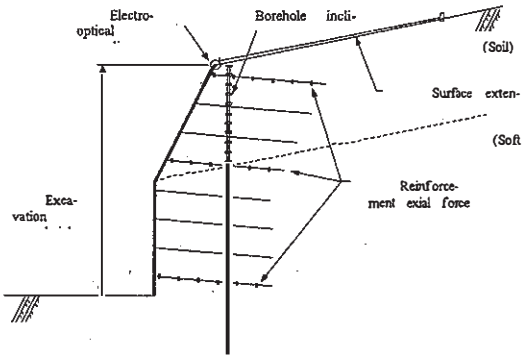

Figure 3.2.1 Example of instrument disposition

(2) Indexes for deformation modes and amount

Deformation modes of excavated surfaces when applying the reinforced slope method are as shown in Figure 3.2.2. They in general collapse forwards, but in some cases of excavation in a gentle slope, swelling and sliding may be induced (Japan Highway Public Corporation. Dec. 1994)..

Figure 3.2.3 (Tayama et. al. 2000) demonstrates displacement on excavated surfaces during work and just before collapsing. In this figure, are shown the test results from a full-scale destruction experiment by applying loading force on the slope 5m high, cut vertically from the top. From this, we learn that forward falling as displacement occurs when excavating, but just before collapsing, the lower portion produces a larger displacement, and the upper portion displaces significantly in the vertical direction. The time span between completion of loading and the moment just before collapsing is 7 minutes and 30 seconds. This indicates that the ground improved

by the reinforced slope method is considerably toughened.

Tayama et. al. (2000) showed relationship between excavation height H and slope top horizontal displacement δ h in Figure 3.2.4, which is determined referring to literatures available and on-site tests. The dotted line in the figure depicts the normalized horizontal displacement δ h/H. Based upon this diagram, The Japan Highway Public Corporation (Oct. 1998) provides reference values for stability management criteria for steep slope excavations (1:0.0 to 1:05). These reference values are graded normal level, warning level and stop level.

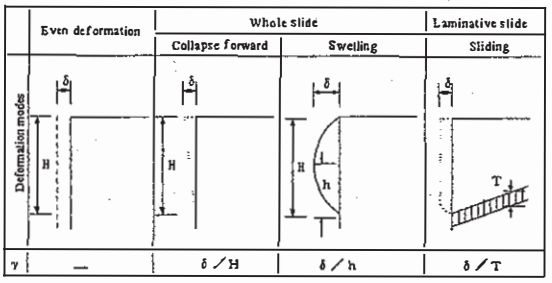

γ : shear strain of rock

Figure 3.2.2 Deformation mode.

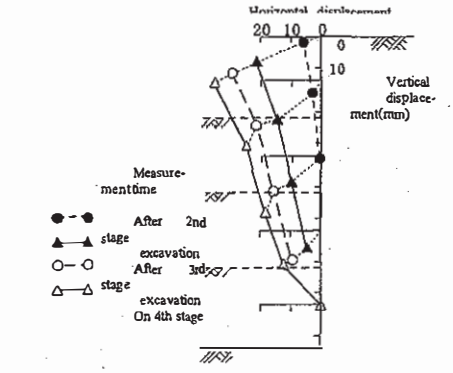

(On excavation, 1:0.0, L=2.5m)

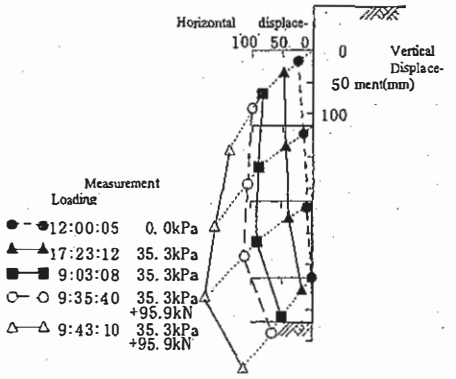

(Just before the fracture, 1:0.0, L=2.5m)

Figure 3.2.3 Displacement of excavated surface

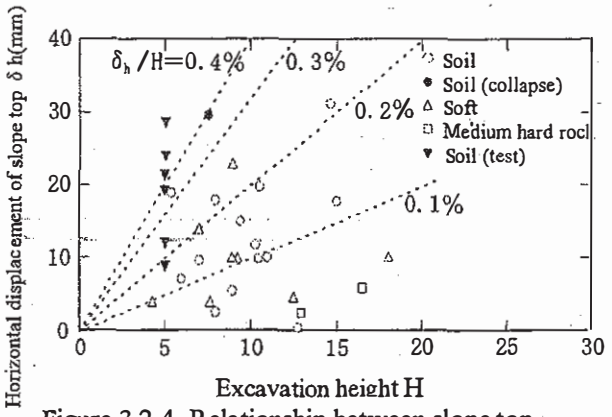

Figure 3.2.4 Relationship between slope top horizontal displacement and excavation height.

3.2.2 Case studies

(1) Long-term measurement cases

In the work by the reinforced slope method, in many cases, deformation measurement is implemented for stability management, but there are few cases continuing measurement of deformation and axial forces for a long period. Table 3.2.3 shows measurement cases, which have been obtained referring to the records available in Japan.

In the Site "a", displacement started emerging immediately after the excavation of the fifth stage (number of excavation stage is six), and converged 14 days after the completion of the excavation. But displacements increased subsequently because of the operation of construction machines and loading of embankment. The displacement amount 2 months later was 21 mm and exhibit converging trend.

Figure3.2.5 demonstrates the Site "e". Ground displacement increased along with advance of excavation, and reached 25 mm at the moment of the completion of excavation. Since then, the displacement had increased slightly for two months, and converged nearly completely, to 31 mm in 4 months, and approximately 34 mm in 24 months. This district underwent an earthquake of 4 degrees on the seismic scale about one year after completion (March 18,1987), but there were no remarkable changes in displacement after the earthquake.

Axial forces measured one month after cutting are available (Matsui et. al. 1990). The tensile forces of reinforcement rods continue increasing gradually even after one month from the cutting.

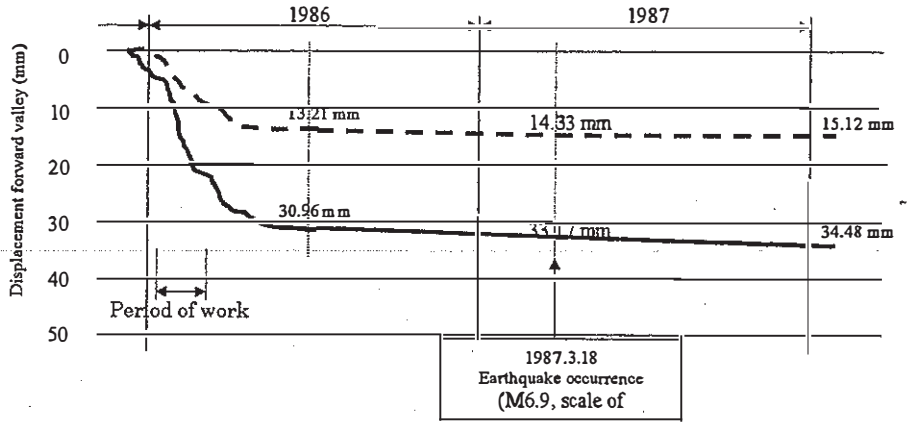

Figure 3.2.5 Ground displacement gauge, change with time of displacement.

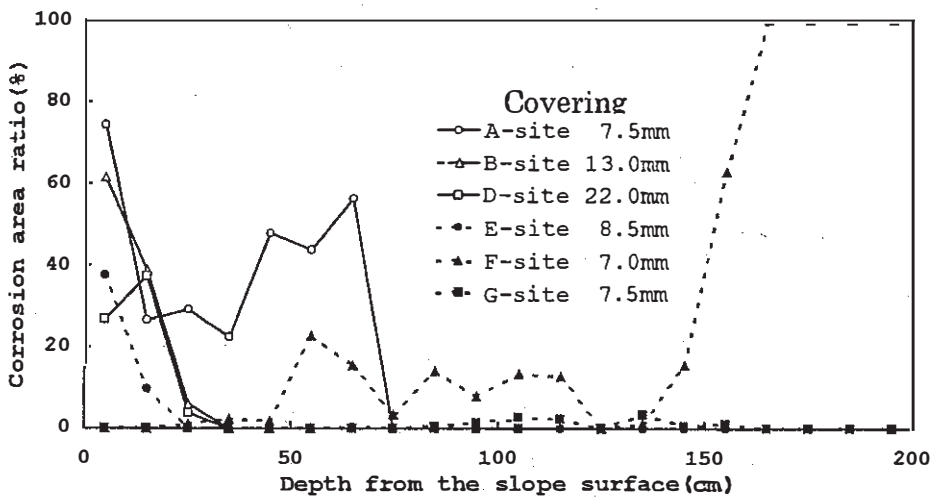

Figure 3.2.6 Distribution of corrosion area ratio.

(2) Long-term durability of reinforcement bars

In overseas, anti-corrosion of reinforcement bars for durability is highlighted as one of important topics (Japanese Geotechnical Sosiety, 1996). For example, a certain paper in France provides classification of anti-corrosion grades per service period and corrosive environments. Endurance periods are classified into three categories, shorter than 18 months, 18 months to 30 years and longer than 30 years, and corrosive environments into 4 categories.

The French standard provides classification of corrosive environments, by totalizing the scores for parameters such as kind of ground, ground resistibility, groundwater and pH value. The said standard proposes admissible corrosion depth, coating and electric plating, plastic coating and use of special steel grades.

In the U.S.A., grout covering and epoxy-based electrostatic coating are used as anti-corrosive means.

In Japan, a survey was conducted on the corrosion of reinforcement bars placed in the sites whose ground was improved 10 years or more before, to evaluate their endurance (Tayama et. al. 1996).

Investigation items include over-coring and material tests. Table 4.4 shows the corrosive condition of reinforcement bars which are placed in the slopes surveyed, and Figure3.2.6 depicts the depth distribution of corrosion area ratio.

The tensile test results of the reinforcement rods show there is no sample whose strength level is lower than the standard. We learn that in Districts A, B, D and E, some corroded samples are found in shallow depths 30 cm or less from the ground surface. As the reason why corrosions occurred at such

Table 3.2.3 Cases of displacement measurements for long period

Site	Vertical height (m)	Gradient	Reinforcement length (m)	Elapsed time (month)	displacement (mm)
a	9.5	1:0.2	5	2	21
b	6	1:0.4	3-7	4	9
c	8	1:0.18	3-7	4.5	12
d	5.3-6.5	Vertical	4.5-5.0	9	10
e	14	1:0.5	3-6	24	34

Table 3.2.4 Corrosion of reinforcement bars.

Survey area	Elapsed time (year)	Geological rock condition	Tensile test		Corrosion of reinforcement rods		
			Yield point (MPa)	Tensile strength (MPa)	Max. corroded area (%)	Max. corroded location	Max. corroded depth
A	10	Mesozoic slightly weathered sandstone	-	555	74	0-10	5.75
B	8	Palaeozoic slightly weathered tuff	363	552	95	0-10	1.75
C	9	Talus cone deposit clayey soil with gravel	392	605	0	–	None
D	9	Palaeozoic Weathered sandstone	353	552	38	10-20	None
E	15	Palaeozoic Sandstone Crystalline schist	415	598	38	0-10	1.40
F	9	Neogene Mudstone,Sandstone	396	588	100	140-190	1.87
G	7	Kanto loam	392	578	9	390-400	0.84
H	10	Neogene Andesite Tuff	-	-	-	-	-
I	9	Mesozoic or Palaeozoic Sandstone,Mudstone	-	-	-	-	-

shallow depths, we can assume that at the moment of grouting, grout material penetrated deep in the ground, and its amount was not enough to fill the upper portion of holes. On the reinforcement rods in Districts A, F and G, corrosion was found deep in the ground. The survey also reveals that reinforcement rods in Districts B, C and D with 10 mm or thicker covering are completely free from corrosion deep in the ground. Therefore, corrosion deep in the ground in Districts A, F and G was due to insufficient covering thickness.

The following are the measure with which we can cope with corrosion of reinforcement rods.

1. Head section of reinforcement bars
   Galvanize head sections of reinforcement.
2. Reinforcement bars near the surface (around the injection hole)
   Injection should be carried out carefully.
3. Reinforcement bars into the ground.

Galvanize reinforcement bars. To ensure a covering on reinforcement bars 10 mm or more, spacer shall be placed at intervals of not more than 2.5mm. In the design, a corrosion margin of 1mm shall be considered.

with a corrosion margin of 1 mm or reducing admissible stress.

REFERENCES

Japan Highway Public Corporation. Oct. 1998. Designing and Construction Procedure for Soil Nailing Method (In Japanese)

Japan Society of Civil Engineers. Dec. 1994. Analysis and Measurement of Stability of Bedrock Slope, p217 (In Japanese)

Tayama,S., Ogata,K., Nagayoshi,T., Takeuchi,T. March 2000. Safety Management by Measurement of Excavated Slope by the Reinforced Slope Method, Proceedings of Japan Society of Civil Engineers, No.644/VI, pp113-122 (In Japanese)

Muramatsu,M., Kitamura,T., Goto,E., Suami,K. Sep. 1991. Cases of Earth Improvement with Reinforcing Bars of Talus Cone, Japan Society of Civil Engineers, Meeting of Reading Research Papers of the 46th Annual Meeting (In Japanese)

Sugiyama,M. Nov. 1991. Cases of Embankment Improved by Reinforcing Bars for Creation of Land, Foundation Work, pp62-67 (In Japanese)

Japanese Geotechnical Society. March 1996. Committee Report of Symposium on the Reinforced Slope Method, pp212-213 (In Japanese)

Fujiwara,T., Hirose,Y., Tateyama,M. March 1996. Excavation for Railway Track Embankment Using Large Diameter Reinforcement, Proceedings of Symposium on Reinforced Slope Method, pp325-330 (In Japanese)

Express Highway Research Foundation of Japan Feb. 1994. Study on Design and Construction of the Reinforced Slope Method of Fiscal 1993 (Part 2) , pp3-145 to 3-149 (In Japanese)

Matsui,T.,San,K.C., Kawada,K., Watanabe,K., Fukuda,Y., Hayashi,K. June 1990. Field Test on a Reinforced Cut Slope in Residual Soil, Proceedings of 25th Research Paper Reading Meeting, pp2049-2050 (In Japanese)

Japanese Geotechnical Society March 1996. Proceedings of Symposium on the Reinforced Slope Method (In Japanese)

Tayama,S., Maeno,K., Matsuyama,H Oct 1996 Research of Durability of the Reinforced Slope Method, Soil and Foundation, pp35-36 (In Japanese)

3.3 *Sismic stability*

3.3.1 *Summary*

The seismic stability is not considered in the design of reinforced slope in the present design rules for the following reasons:

(a) Execution sites we normally on the comparatively stable ground; and
(b) Reinforced slopes have been damaged by rainfall rather than by earthquakes.

However, there were some damaged (or deformed) slopes by the 1995 Hyougoken-Nambu Earthquake. This suggests that a seismic design rules are required.

This section introduces the seismic characteristics of reinforced slope based on the report on the damage caused by the Hyougoken-Nambu Earthquake, model tests and numerical analyses.

3.3.2 *Case studies*

Some reinforced slopes were damaged by the Hyougoken-Nambu Earthquake. Two reports on reinforced slopes in the Hyougo area are introduced.

(1) Disaster researches

The authors of this report investigated 10 sites of within the area 70km from the hypo-center. The reinforced slopes in these sites are constructed by the "root-pile method." Figure 3.3.1 shows the deformation of reinforced slopes classified by the maximum acceleration and the height of structure. According to this figure, there is no correlation between the deformation and the maximum acceleration or the height of structure. Therefore, the deformation may have been caused by different conditions of ground, length of reinforced bar, stiffness of wall and other factors.

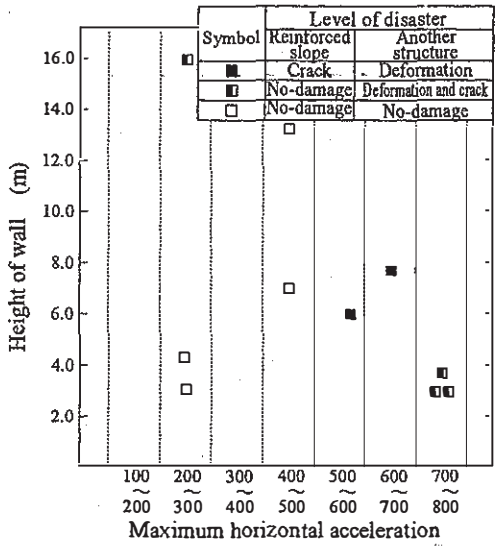

Figure 3.3.1 Level of disaster based on the height of wall and the maximum horizontal acceleration

(2) Roads on the Awaji Island

This construction of the connection road for the Chama river on the Awaji island was constructed by the reinforced slope method. The original ground mainly consists of granite. The dimensions of the reinforced slope are: wall height 16m, wall gradient 1:0.2; and deformed reinforced bar (SD295A) length 3.0 to 7.0m. The pitches of reinforced bars are 1.5m and 1.4m. Two ground anchors are used to prevent the growth of deformation, since the bars deformed during the construction work.

The reinforced slope is constructed by using three materials, the reinforced bars, shotcrete (150mm thickness), and concrete facing. The cross-section of this reinforced slope is showed in Figure 3.3.2. This figure is not drawn the bridge abutment. This abutment, which is 6.4m high, and is constructed in front of the reinforced slope. This reinforced slope was not damaged by the horizontal acceleration, about 600gal, of Hyougoken-Nambu Earthquake in this area.

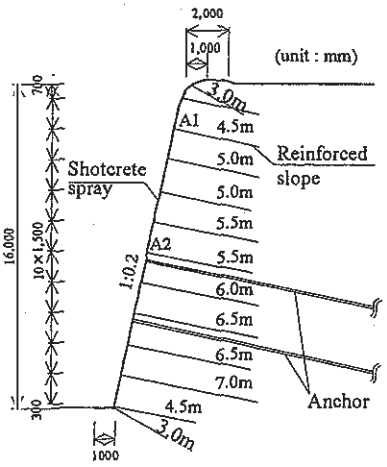

Figure 3.3.2 Cross-section of a slope for a road on the Awaji Island.

3.3.3 *Model tests*

In this section, we introduce the results of two shaking table tests performed under contrifugal and gravity conditions.

(1) *Model test under the contrifugal condition*

This test was implemented to estimate the seismic stability of reinforced slope with reinforced columns. The test conditions and used materials are as follows:

(a) Model ground: DL clay
Water content: 20%
Unit volume weight: 14kN/m^3;
(b) Reinforcement: strings of guitar
Diameter: 0.58mm;
(c) Grouting: silicon glue, plaster;
(d) Other condition: 50G
(the model size is 1/50 of the original model);
(e) Reinforced slope model
Height: 140mm
Slope gradient: 1:0.3
Internal of reinforcements: 30mm.

Table 3.3.1 Case of tests

Case	diameter of reinforcement (mm)	material of grouting	length of reinforcement (mm)	cover of slope surface
3	non-reinforcement			
4	2	bond	80	no
5	2	bond	80	setting
6	7	gypsum	80	setting
7	7	gypsum	40	setting

This test was to estimate the effect of the diameter and length of reinforcement and the length of reinforcement, the slope cover (OHP sheets) to prevent disturbing local fracture. The test cases are shown in Table 3.3.1. The test model is shown in Figure 3.3.3. The items of measurement are the horizontal displacement of the slope surface, the vertical displacement of the back ground and the acceleration of the reinforced slope. The wave used for the test was a sine wave at the frequency of 100Hz. A 4-step wave was input into maximum acceleration of 60, 120, 150, 150gal. The numbers of 1step wave are 20cycles except of the forth step. Only the forth step wave is 40cycles.

Figure 3.3.4 shows the settlement of slope surface wave at the maximum acceleration of 120gal was input. This Figure compares the difference in the

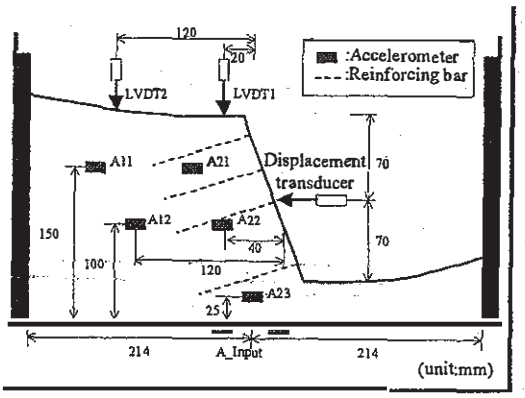

Figure 3.3.3 Test model

settlement at differs reinforcement diameters. When large diameter reinforcement bar are used, the settlement is smaller. The relation between the input seismic energy and accumulating settlement is shown in Figure 3.3.5 as the parameter of seismic energy, the Arias Intensity (Ia) was used. According to pull-out tests of reinforcement in the past, the reinforcement strength reaches a peak, when the pulled displacement is about 2mm. When the pulled displacement was about 2mm, the slope edge settlement was about 100mm. From the test results of cases 4 and 5, the settlement increased quickly after the reinforcement strength reached a peak.

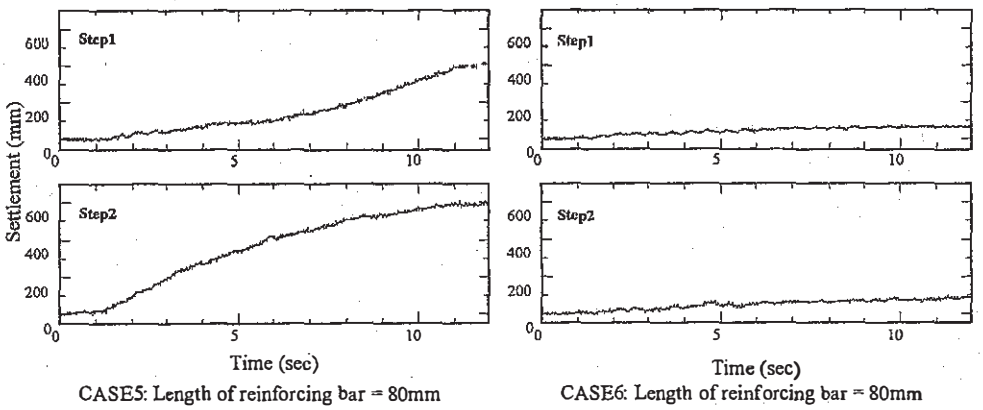

Figure 3.3.4 The settlement of slope edge

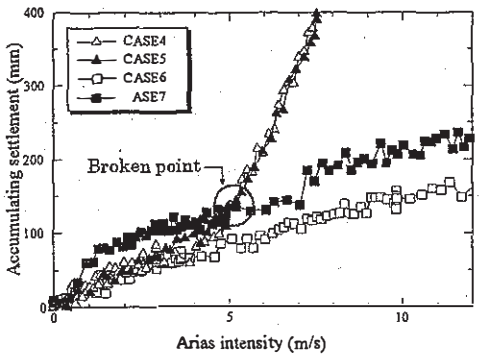

Figure 3.3.5 Relation between the input seismic energy and accumulating settlement

(2) *Model test under the gravity condition*

We describe a shaking table test under the gravity condition. The experiment model size was 1/10. Two types of back ground, stable soil and unstable soil, were used. An example of cross-section of test model is shown in Figure 3.3.6. We investigated the relation between the reinforced slope and leaning type retaining wall to estimate the reinforcement effect.

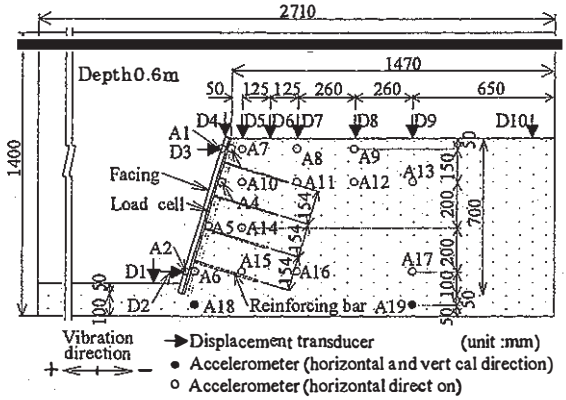

Figure 3.3.6 Test model

Table 3.3.2 Character of materials

structure	material	character
ground	Inagi-sand	γ_d=13.32(kN/m^3) w=21.0(%)
cobble stone	small ballast	γ_d=16.12(kN/m^3) d_{AV}=2-10mm
facing	duralumin	714×514× 40mm
reinforcement (long length)	phosphor bronze	ϕ 5.5×300mm
reinforcement (short length)		ϕ 5.5×150mm

(a) Experiment of reinforced slope of stable soil

As the stable soil, we used the Inagi sand at the optimum water content. After the stable soil was prepared, the reinforcement was set up along the guide hole and the wall was constructed. Model materials are shown in Table 3.3.2.

We used a sine wave of 5Hz. We input a step wave at maximum acceleration intervals of 50 gal (stating at the acceleration of 50gal). Duration of one step was 10 minutes. Four test cases were carried out as shown in Table 3.3.3.

The leaning type retaining wall in the case1 broke at 450gal to accumulate the deformation of the settlement of cobble stone. The facing in the case2 did not break at 1000gal at the end of experiment. But

Table 3.3.3 Case of tests

Case	form
1	facing and cobble stone
2	only facing
3	facing and long reinforcement
4	facing and short reinforcement

Table 3.3.4 failure accelerations of each case

case	failure acceleration
1	75gal～150gal
2	200gal～250gal
3	300gal～350gal
4	600gal

the facing vibrated. The reinforced slope in the cases3, 4 were stable at 1000gal at the end of experiment. We confirmed the seismic stability of reinforced slope by these shaking table tests. In the case of stable soil, short reinforcements have a sufficient reinforcement effect.

The contour of acceleration at the end of experiment is shown in Figure 3.3.7. Only the facing part showed high response in the cases 1 and 2. The facing and back ground showed the same response in the cases 3 and 4. From these shaking test results, we understand that reinforced slopes have high seismic resistance.

(b) *Experiment of reinforced slope of unstable soil*

We discussed to carry out the case of reinforced slope constructed on the unstable soil. The Toyoura sand was used as the material forth model of unstable soil used Toyoura sand. The test condition and the test case were the same as in the case of stable soil shown in Tables 3.3.2 and 3.3.3.

Acceleration to break the reinforced slope in each case is shown in Table 3.3.4. Figure 3.3.8 shows the contour of acceleration. The seismic resistance of the reinforced slope increased to about 2 to 4 times that of the leaning type retaining wall. But the seismic effect of short reinforcement (case 4) was lower than that in the case of stable soil. We understood that reinforced slopes of unstable soil require long reinforcement bars. The responded acceleration increased at the edge of reinforced slope. This result was especially remarkable in the case 1.

We described two shaking table tests. From the test results, it can be concluded that the seismic resistance of the reinforced slope is larger than that of the leaning type retaining wall.

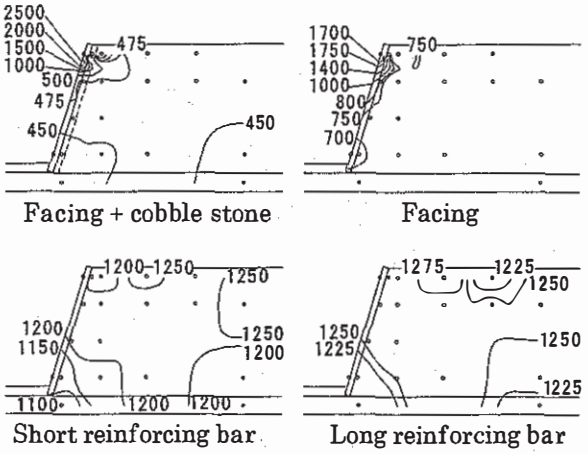

Figure 3.3.7 Counter of response acceleration

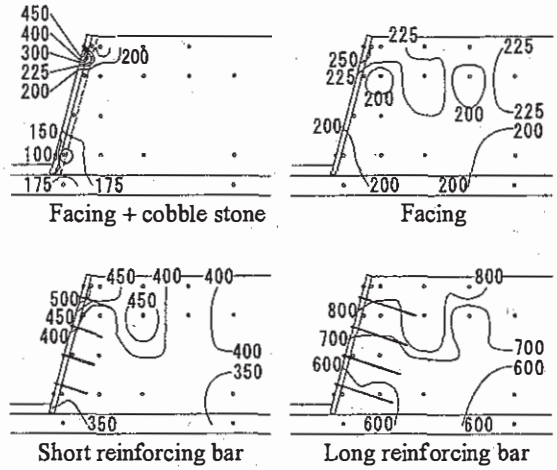

Figure 3.3.8 Counter of response acceleration

3.3.4 *Numerical analyses*

(1) *Seismic stability analysis by response analysis*

Two numerical analyses to estimate the seismic character are described below:

(a) The first method is to analyze the seismic intensity with a constant reinforced slope model (seismic coefficient method); and

(b) The second method is to analyze the seismic intensity with a reinforced slope model is obtained by responded analysis (modified seismic coefficient method).

The authors performed dynamic analyses. The analysis model was shown in Figure 3.3.9. The analysis modeling is as follows. The ground model is a plain strain element, and the reinforcement model is liner bar element. The center value of Seed and Idriss relation was need as the non-liner parameter of sand (reinforced slope part). The frequency response analysis was performed (equivalent liner method) by using two-dimensional finite element method. The input wave is EL CENTRO wave and the maximum accelerations were 70, 100 and 200gal. The boundary of the depth direction is twice the length of reinforced slope height. The energy transmission boundary was set as the boundary condition of the model side.

As an example of analysis results, the distribution of response acceleration in the height direction is shown in Figure 3.3.10 (at the input wave acceleration of 200gal). The response acceleration at the part of edge of reinforced to slope increased about 1.5 to 2.0 times that at the part of the ground of reinforced slope. For the stability analysis, we set the internal friction angle at =25 ° , cohesion at =20.6kPa . The result of stability analysis is shown in Table 3.3.5. The safety of the method (b) decreased (by) 0.11-0.14 from that of the method (a).

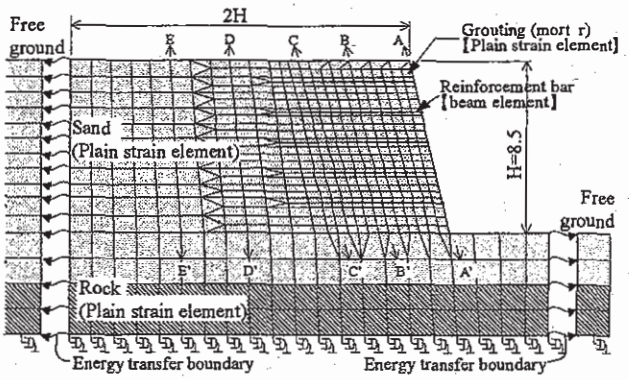

Figure 3.3.9 Analysis model.

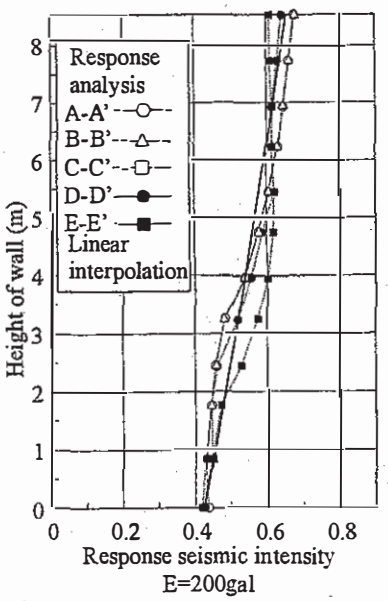

Figure 3.3.10 Distribution of response acceleration

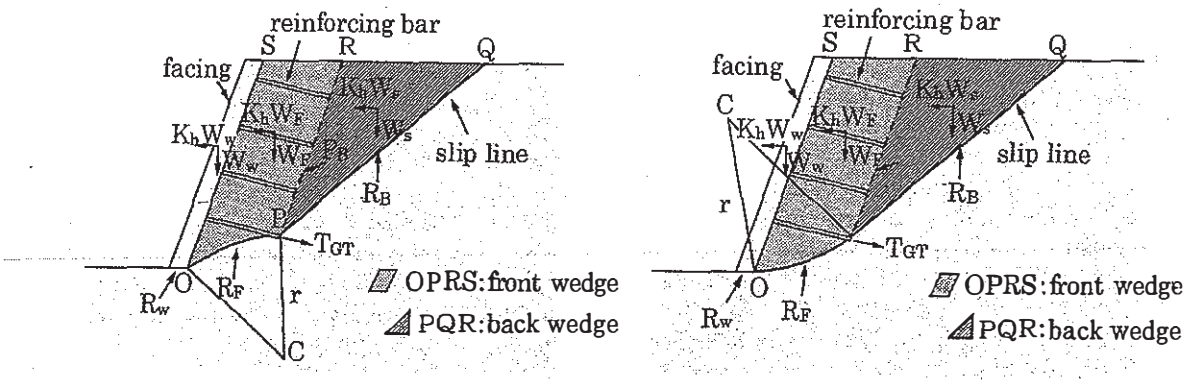

Figure 3.3.11 Failure mode

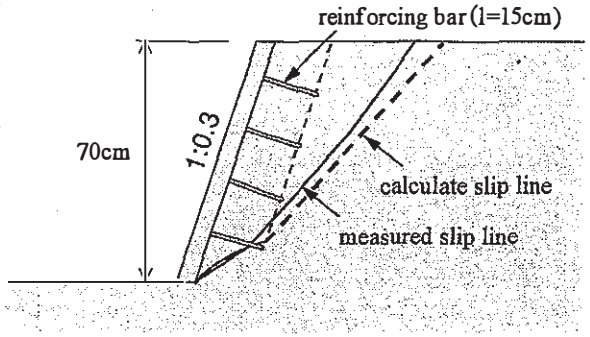

Figure 3.3.12 Result of stability analysis.

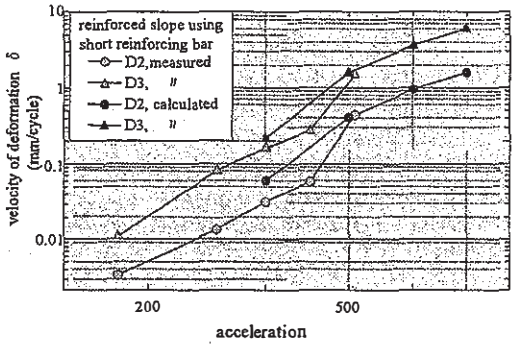

Figure 3.3.13 Relation between acceleration and deformation velocity

Table 3.3.5 safety factors of seismic coefficient method and modified seismic coefficient method

seismic force	0	70	100	200
safety factor	Fs			
seismic coefficient method	1.2	1.137 (0.154)	1.056 (0.214)	0.810 (0.427)
modified seismic coefficient method	1.2	1.020 (0.17-0.29)	0.918 (0.24-0.38)	0.648 (0.46-0.63)

( ) : seismic coefficient used in calculation

(2) *Residual deformation analysis*

The seismic design of soil structures requires, not only stability analysis but also deformation analysis. In this section, we show the calculation result of residual deformation in a shaking table test of reinforced slope.

The method of residual deformation analysis was as follows. Two failure modes were set. One was the sliding mode and the other is the overturning mode (Figure 3.3.11). The displacement was obtained by integral of the following formula.

$$J\ddot{\theta} = M_d - M_r$$

$\ddot{\theta}$: angular acceleration
J : moment of inertia
M_d : moment of rotation
M_r : moment of resistance

The slip line was assumed as the critical slip line (safety factor = 1.0). The conditions of analysis were: height of reinforced slope 0.7m, thickness of concrete facing 0.04m, unit volume weight of facing 27.4kN/m^3, unit volume weight of soil 15.6kN/m^3, internal friction angle 51° , the diameter of reinforced bar 5mm and construction angle of reinforcement 20° . Only the overturning was occurred, since the model broke in this mode.

The result of stability analysis is shown in Figure 3.3.12. The failure seismic coefficient is 0.257. The residual deformation was calculated by using the critical slip line of the result of this stability analysis. The input wave was a sine wave at the frequency of 5Hz. A step wave was input at intervals of 100gal from 300gal to 600gal. The relation between acceleration and deformation velocity is shown in Figure 3.3.13. This Figure shows that the calculation result agrees with the experiment result.

3.3.5 *Remarks on seismic stability of reinforced slopes*

We introduced the seismic resistance of reinforced slope based on a recent research of the site measurement model tests and numerical analyses. From these research and tests, we conclude that reinforced slopes have high seismic resistance.

The method for seismic estimation of reinforced slope is shown in Table 3.3.6. Model tests were performed under two conditions. One was contrifugal

and other condition was gravity conditions. There are several precautions in creating models (material, soil and other conditions). The seismic design of soil structure requires not only the stability analysis to use mainly L1 design but also deformation analysis to use L2 design. There are two cases in the stability analysis. One is the seismic coefficient method, and the other is the modified seismic coefficient method, that give different results. Designers need to choose the optimum method. The residual deformation analysis method in this paper assumes a rigid slip. Therefore, the slip line is determined by stability analysis. A more detailed method is the one to use the finite element method. But this method is very complex. The method of numerical analysis requires further development and studies. We need to establish the seismic design of reinforced slope based on these researches.

Table 3.3.6 Researches of seismic estimation (reference 3.3-4.5.6.7)

study method	classification	application
model test	gravity condition	· 1/10 model · sand
	contrifugal condition	· 1/50model · clay
numerical analysis	stability analysis	· safety facter · seismic coefficient method · modified seismic coefficient method
	deformation analysis	· deformation · rigid plastic analysis · elasto-plastic analysis (using the F.E.M.)

4 CONCLUSION

The authors searched reports of researches and observations on long-term performance and seismic stability of reinforced soil structures published mainly in Japan.

In most of long-term observations, for both of reinforced embankment and reinforced slopes, their measurement periods are several weeks to several months limited within the construction periods, and the behaviours after construction and during service were observed in only few cases. Although it often takes high cost, careful and detailed observations of long-term behaviours of structures are essential for development of more reasonable design and construction methods, including limit state designs. As for the numerical analysis, only the behaviours due to the load increment during construction are analyzed in most cases. Analysis based on time-dependent characteristics of the soils and reinforcing materials are very few.

Several seismic design methods have been established for reinforced soil embankments and walls. The performances of the structures observed in the damaged sites of the 1995 Hyogoken-Nambu Earthquake and others have shown that they are seismically stable enough if properly designed and constructed. However, more reasonable and economical design and construction methods may be possible. As for reinforced slopes, no seismic design method is employed in general, possibly because most of reinforced slopes are constructed on relatively stable natural grounds at the present. Seismic stability of reinforced slopes can be a new research topic in future.

REFERENCES

Fujii,T. Sueoka,T. Muramatsu,M. Mega,M. Ohtani,Y. 1996. Behaviour of soil nailed walls and rootpiles structures caused by the 1995 Hyogo Nambu Earthquake. *Proceedings of Symposium on Reinforced Slope*, pp.295-298. (in Japanese)

Tsukuda,T. Yamamoto,A. Fukuda,N. 1996. Stability analysis of cut slope reinforced with steel bars at north area of Awaji island during Hyogoken-Nambu Earthquake. *Proceedings of Symposium on Reinforced Slope, pp.291-294.* (in Japanese)

Izawa,J. Kusakabe,O. Takahashi,A. Tayama,S. Takamoto,M. 2000. Centrifuge model tests on seismic stability of reinforced cutting slope. *Proceedings of The Thirty-fifth Japan National Conference on Geotechnical Engineering, Volume2*, pp.2197-2198. (in Japanese)

Kimura,H. Yonazawa,T. Kitagawa,S. Aoki,H. Tateyama,M. 1998. Shaking table test of retaining wall leaned on stable soil. *Proceedings of The Thirty-third Japan National Conference on Geotechnical Engineering, Volume2*, pp.2433-2434. (in Japanese)

Yonezawa,T. Kitagawa,S. Aoki,H. Tateyama,M. Kojima,K. Horii,K. 1998. Shaking table test of retaining wall leaned on unstable soil. *Proceedings of The Thirty-third Japan National Conference on Geotechnical Engineering, Volume2*, pp.2435-2436. (in Japanese)

Ezaki,J. Fukuda,N. Yamamoto,A. Tayama,S. 1996. A study of seismic stability for reinforced slope. *Proceedings of Symposium on Reinforced Slope*, pp.299-302. (in Japanese)

Horii,K. Aoki,H. Yonezawa,T. Kitagawa,S. Akita,K. Tateyama,M. 1998. Permanent residual deformation analyses of retaining wall with soil nail. - verification for shaking table test of retaining wall - *Proceedings of The 53th Annual Conference of The Japan Society of Civil Engineers, 3(B)*, pp.488-489. (in Japanese)

Seed,H.B., Idriss,I.M. 1970. Soil moduli and damping factors for dynamic response analysis, *Report No.EERC 70-10*, University of California.